1-1-2015

Accurate And Efficient Reliability Analysis Of Complex Structural Engineering Problems

Kapil Dilip Patki
Wayne State University,

ACCURATE AND EFFIICIENT RELIABILITY ANALYSIS OF COMPLEX STRUCTURAL ENGINEERING PROBLEMS

by

KAPIL DILIP PATKI

DISSERTATION

Submitted to the Graduate School

of Wayne State University,

Detroit, Michigan

in partial fulfillment of the requirements

for the degree of

DOCTOR OF PHILOSOPHY

2015

MAJOR: CIVIL ENGINEERING

Approved By:

_____
Advisor   Date

_____

_____

DEDICATION

I would like to dedicate my work to my mother
for her countless sacrifices and
to my beloved wife for her continuous support.

ACKNOWLEDGMENTS

TABLE OF CONTENTS

LIST OF TABLES

LIST OF FIGURES

NOMENCLATURE

CDF   Cumulative Distribution Function (F_x)

EGLD   Extended Generalized Lambda Distribution

FS   Advanced Failure Sampling

GEV   Generalized Extreme Value Distribution

GLD   Generalized Lambda Distribution

JSD   Johnsons Distribution

MCMC   Markov Chain Monte Carlo Method

MCS   Monte Carlo Simulation

NI   Numerical Integration

PDF   Probability Density Function (f_x)

RV   Random Variable

f_g PDF of g; also, PDF of the GLD (eq 4)

f_Q PDF of Q

F_R CDF of $R(X_j)$

f_R PDF of $R(X_j)$

$g(X_i)$ initial limit state function

g^* FS limit state function

p_f failure probability

Q   control RV

q   a specific value of Q

$R(X_j)$ resistance function

R	$R(X_j)$ represented as a single equivalent resistance RV
β	reliability index
λ_i	GLD parameter
Φ	standard normal CDF
Γ	transformation function of JSD
γ, δ	shape parameter for JSD
ξ	location parameter for JSD
λ_j	scale parameter for JSD
k	shape parameter for GEV
μ	location parameter for GEV
σ	scale parameter for GEV

CHAPTER 1 INTRODUCTION

Reliability Analysis

Uncertainties are unavoidable while dealing with various civil engineering problems. These uncertainties are often referred as random variables (RV) (non-deterministic quantities) and are usually modeled and formulated using the concepts of probability and statistics. Reliability analysis is the study of effect of these uncertainties on the design and performance of a system. In civil engineering, reliability is defined as the probability that the structure will serve within a specified limit or probability of occurrence of specified events; usually 'failures'. In concept, a multidimensional integration of the joint probability density function (PDF) over the entire failure domain is conducted to determine the probability of failure. However, solving this multidimensional integral is a complex task.

To avoid the aforementioned difficult task, researchers have developed various alternative techniques to determine the probability of failure. From past research, the structural reliability analysis techniques can be generally categorized into two groups; simulation methods and reliability index-based methods (β-based methods). Simulation methods are the oldest methods in reliability analysis and are based on randomly simulating a phenomenon and counting the occurrence of the event of interest (Nowak and Collins 2000). Monte Carlo Simulation (MCS) is the most popular and simplest simulation based method. MCS has the potential to solve complex physical as well as mathematical problems with high accuracy. Although potentially accurate and simple to implement, the computational cost of MCS while evaluating complex engineering

problems with low failure probability may be infeasibly high. To reduce the cost of MCS but maintain reasonable accuracy, numerous variance reduction techniques (VRT) were developed such as stratified sampling (Iman and Conover 1982), importance sampling (Rubinstein 1981; Engelund and Rackwitz 1993) and adaptive importance sampling (Wu 1992; Karamchandani et al. 1989). However, stratified sampling techniques such as Latin Hypercube (Iman and Conover 1982) have not consistently shown significant reductions in computational costs, and for importance sampling methods they rely on identifying the most probable point of failure (MPP), may also fail to provide solutions for complex limit states. Various other simulation methods that do not rely upon the MPP have been proposed, such as subset simulation (Au and Beck 2001; Au et al. 2007), directional simulation (Ditlevsen and Bjerager 1988), and the modified conditional expectation methods (Eamon and Charumas 2011), among others. However, many of these alternative methods have been rarely used in the technical literature. Rather than refine the reliability method, a response surface (RS) technique can be used to represent a computationally expensive limit state function with a simpler, analytical surrogate function (Gomes et al. 2004; Cheng et al. 2009). Once formed, the response surface can be used to provide very fast reliability solutions. However, these techniques often require high computational effort to develop accurate responses for highly non-linear or discontinuous limit state functions, a cost which may outweigh the saving gained with their use (Eamon and Charumas 2011).

The other group of structural reliability analysis techniques, β-based methods, are analytical approximation techniques and uses the concept of reliability index, a surrogate

measure of probability of failure. Cornel (1969) developed the first beta-based method called the First Order Second Moment Method (FOSM). However, FOSM was only applicable to normal RVs and also yielded different results when the limit state function was re-written in different mathematical forms, the latter deficiency known as the 'invariance problem'. This issue was solved by Hasofer and Lind with the Advanced First Order, Second Moment Method (AFOSM) (Hasofer and Lind 1974). Later, the First Order Reliability Method (FORM) was developed by Rackwitz and Fiessler in 1978 which addressed the use of non-normal RVs. Although superior to FOSM and AFOSM in this regard, FORM still suffered inaccuracy problems for problems highly non-linear in standard normal space. Fiessler (1979) and Breitung (1984) later addressed this issue by introducing a new method; the Second Order Reliability Method (SORM). SORM differed with FORM by developing a curvilinear failure surface at the most probable point of failure (MPP) rather than the previous first order, or linear, fit. However, SORM still remains an approximate representation of the actual failure boundary, and inaccurate assessment of failure probability may exist for highly nonlinear problems. A fundamental problem with all of the aforementioned β-based methods is that they rely on identifying the MPP on the failure boundary. Although computationally efficient, these methods may provide poor solutions for problems nonlinear in standard normal space caused by the linearization of the limit state function at the MPP (Eamon et al. 2005, Melchers 1999; Chiralaksanakul and Mahadevan 2000, Haldar and Mahadevan 2000). Moreover, search algorithms sometimes cannot identify the MPP for complex problems that may be highly non-linear, discontinuous, or that have multiple 'local' MPPs on the

failure boundary (Eamon and Charumas 2011). In such cases, the reliability-index based methods may fail to provide any solution.

Other reliability analysis methods such as point estimation and point integration techniques (Rosenblueth, 1981 and Zhou, 1988) were also developed and cannot be categorized based on the above mentioned two groups. However, the results obtained through these methods may be highly unreliable.

Motivation

The current state-of-the-art in reliability analysis leaves a significant category of problems that are not readily approachable with the available methods described above. These problems are those of large computational costs and complex limit states for which the MPP cannot be identified accurately. For this class of problems, MCS as well as advanced simulation-based methods are often too computationally costly to apply. On the other hand, β-based methods lack sufficient accuracy or cannot be applied at all. Examples of these problems may include crash and impact analysis, metal forming, and structural systems defined by multiple member failures, etc. Three examples of such problems are described in Chapter III of this dissertation report. Currently, these problems are typically approached by greatly simplifying the response or the reliability analysis. However, such simplifications may lose critical model fidelity and suffer unacceptable inaccuracies in the reliability calculation (Rais-Rohani et al. 2010; Eamon 2007; and Eamon and Rais-Rohani 2008).

The motive behind this research is to address the aforementioned concerns and develop a new reliability approach specifically suited to accurately solve complex

problems of the type described above, with reasonably low computational effort. As analyses of state-of-the art problems involving phenomenon such as blast response, impact and crash safety, and structural system behavior of advanced materials become increasingly complex and demand greater computational costs, similar advances in reliability analysis are needed to enable accurate probabilistic solutions of these problems. In this research, a new approach is proposed to achieve this and is referred to as 'Advanced Failure Sampling' (FS). The basic crude concept of this method was first introduced by Eamon and Charumas (2008). However, the method was found to be inconsistent with regard to accuracy and solution feasibility. That is, although few problems could be efficiently solved, some problems could not, providing worse solutions than desired. Moreover, for some problems, FS could provide no solution at all. However, no guidance is currently available in the literature to allow identification of these types of problems. This is a critical shortcoming as it significantly limits the practical usefulness of FS. As noted earlier, the primary purpose of this research is to address this issue and develop an enhanced version of FS that provides viable, accurate, and efficient solutions to all problems. This research deeply explores three aspects of FS method; development of optimal algorithm for PDF construction of resistance samples, determination of the most efficient method to generate the resistance samples and validation of FS method. These three aspects and exploring various methods to obtain respective possible solutions are discussed and described in detail in Chapter III of this dissertation report. The method will be evaluated for various complex implicit and explicit limit states of structural reliability including those problems requiring finite

element analysis. Few of these problems are described above. The results obtained from the FS method shall then be compared to the results obtained from existing methods such as MCS, FORM, SORM etc. as discussed above.

This research report is composed of six chapters including this chapter:

Chapter II: This chapter explains in details the general concepts of reliability index and reviews the available literature on reliability analysis techniques and their respective drawbacks.

Chapter III: This chapter explains the method development of Advanced Failure Sampling and its algorithm in detail. It also discusses the various techniques implemented to enhance the FS method.

Chapter IV: This chapter presents a database of various complex limit state functions and practical engineering problems which will be evaluated using the FS method to test its effectiveness.

Chapter V: This chapter presents the FS solutions for problems described in Chapter IV and compares it with results obtained with currently available techniques.

Chapter VI: This chapter gives a summary, conclusion and recommendations for use of the FS technique.

CHAPTER 2 LITERATURE REVIEW

Review of Structural Reliability

Structural reliability as a method can be defined as the assessment of the probability of occurrence of 'failures'. Here failure could be any event specified by the analyst. In structural engineering the failure criterion is usually expressed in terms of a limit state; which is a boundary between the desired and undesired performance of a structure. The limit state boundary is often expressed in a mathematical form using random variables (RV) and is formed by setting the limit state function or performance function equal to zero.

In structural reliability, the limit state can be expressed in different ways. Some common ways include:

1. Ultimate Limit States: This type of limit state usually describes a relation between resistance of a structure and the applied load. Following are a few examples:
   - Ultimate moment carrying capacity
   - Formation of plastic hinge
   - Compressive and tensile stress
   - Buckling
   - Rupture
2. Serviceability Limit States: This type of limit state is usually expressed in terms of the deformation of the structural components. For example:
   - Excessive Deflection
   - Excessive vibration
   - Cracking
   - Permanent Deformation

3. Fatigue Limit State: This limit state describes loss in strength due to loads repetitive in nature. Under fatigue the structure can develop cracks which may propagate until rupture.

As mentioned above, the limit state is often expressed in the form of a mathematical expression using RVs. In structural reliability, these RVs are usually categorized as resistance RVs or load RVs and are symbolized as 'R' and 'Q' respectively. For a given failure mode, a common way of expressing a limit state function or a performance function; *'g'* is as follows:

$$g(R,Q) = R(x_i) - Q(x_j) \tag{2.1}$$

where x_i and x_j represent a vector of resistance and load random variables. The boundary between desired (safe) and undesired (failure) performance corresponds to a condition of $g = 0$. The structure is safe if $g \geq 0$ and unsafe if $g < 0$. The probability of occurrence of an undesired performance is termed as probability of failure and is given as follows:

$$p_f = P(R - Q < 0) = P(g < 0) \tag{2.2}$$

Since the limit state is a function of RVs *R* & *Q*, the probability of failure *P(g < 0)* is obtained by conducting a multidimensional integral of the joint probability density function (PDF) of *R* and *Q*, $f_{RQ}(R,Q)$ over the entire failure domain. Following is the expression for the same:

$$p_f = P(g < 0) = \int_{g<0} \cdots \int f_{RQ}(r,q)drdq \tag{2.3}$$

Here $f_{RQ}(R,Q)$ is a joint PDF and has an arbitrary distribution whereas, *g < 0* is the failure domain and may be irregular with a highly non-linear boundary. Hence, evaluation of this probability is often very difficult which leads us to the concept of

reliability index. Reliability index is a surrogate measure of probability of failure and can be determined through both simulation-based and β-based reliability analysis techniques. These techniques are discussed in detail in the following sections.

Simulation Based Methods

Simulation is based on the concept of numerically simulating a phenomenon and counting the occurrence of the event of interest. Most of the simulation based methods are based on MCS which discretizes the multidimensional integral by random sampling. The method is simple and straightforward and can be theoretically applied to any problem. However this method is computationally expensive while dealing with complex problems having low failure probability. MCS, Stratified Sampling (SS), Latin Hypercube Sampling (LHS), and Importance Sampling are a few examples of simulation-based methods and are described in the following sub-sections.

Monte Carlo Simulation (MCS)

MCS is one the most basic and simplest simulation methods and is used for a wide variety of problems. Basically MCS discretizes the multidimensional integral by random sampling. It gives an approximate solution to equation (2.3). In MCS, 'n' independent samples of the vector of resistance and load random variables $R(x_i)$ and $Q(x_j)$ are generated from the joint PDF of $f_{RQ}(R,Q)$. During each sample run or simulation the limit state outcome $g(R, Q)$ is recorded and if $g(R,Q) < 0$, a failure is recorded. The ratio of total number of failures to the total number of samples 'n' is used as the probability of failure p_f estimate. The following is the stepwise procedure of MCS method.

1. Determine the limit state function and the number of RVs.

2. Generate RV values for all RVs such that the probability of getting a particular value is proportional to the PDF of that RV.

3. Insert the RV sampled values into the limit state and then evaluate the limit state. This typically completes one simulation for the given problem.

4. Run a sufficient number of simulations i.e. repeat steps 1-3 a sufficient number of times. The greater the number of simulations, the higher the accuracy of the result.

5. Traditionally, p_f is directly calculated from the results as:

$$p_f = \frac{1}{n} \sum_{i=1}^{n} I_i \qquad (2.4)$$

where:

n = total number of simulations

I_i = Indicator function

$I_i = 1$ if $g < 0$ (failure)

$I_i = 0$ if $g > 0$ (survival)

Reliability index β is obtained from p_f using the following transformation:

$$\beta = -\Phi^{-1}(p_f) \qquad (2.5)$$

The aforementioned process clearly indicates that for low p_f values, a large number of simulations is required. In the case of complex engineering problems this requires higher computational effort and cost. For example, consider a structural member with a typical reliability index β of 3.5, which corresponds to a failure probability p_f of approximately 0.233 × 10-3 (about 1 in 4000). If the problem is solved with traditional MCS using n

samples, the uncertainty in the solution, as measured by the coefficient of variation (COV) of the calculated p_f, can be estimated with (Nowak and Collins 2000):

$$COV(p_f) = (\frac{1 - p_f}{n\,p_f})^{0.5} \qquad (2.6)$$

According to the above expression, to estimate a problem with $\beta = 3.5$ with an uncertainty in the solution no greater than 10% COV requires approximately 429,000 simulations. If the analysis depends on a finite element analysis (FEA) for solution, and only requires 1 minute of CPU time per simulation, the reliability problem would require approximately 7150 CPU hours.

In order to deal with this issue, variance reduction techniques (VRT) were introduced. These methods made adjustments to MCS in an attempt to decrease the number of simulations but retain the same level of accuracy i.e. reduce the variance in the solution. Importance sampling and Latin Hypercube Sampling are a few methods which fall under this family and are described below.

Importance Sampling

As noted earlier, if the p_f is small, most of the MCS simulations do not fall in the failure domain. Importance sampling addressed this problem with increasing the number of failures by using a sampling distribution $h_X(x)$ having more probability content in the region $g < 0$. However, sampling in the failure region requires identifying the most probable point of failure (MPP). This is usually achieved by using the β-based reliability analysis techniques. Figure 2.1 shows a schematic representation of the importance

sampling method. The failure probability computed using importance sampling can be described using the following expression:

$$p_f = \frac{1}{n} \sum_{i=1}^{n} I(g \leq 0) \frac{f_x(x)}{h_x(x)} h_x(x) \qquad (2.7)$$

where:

I = Indicator function

(x) = random sample taken from the distribution of $h(x)$

$f_x(x)$ = PDF of sample x, based on the original RV parameters

$h_x(x)$ = PDF of sample x, based on RV parameters of $h(x)$

n = number of samples taken
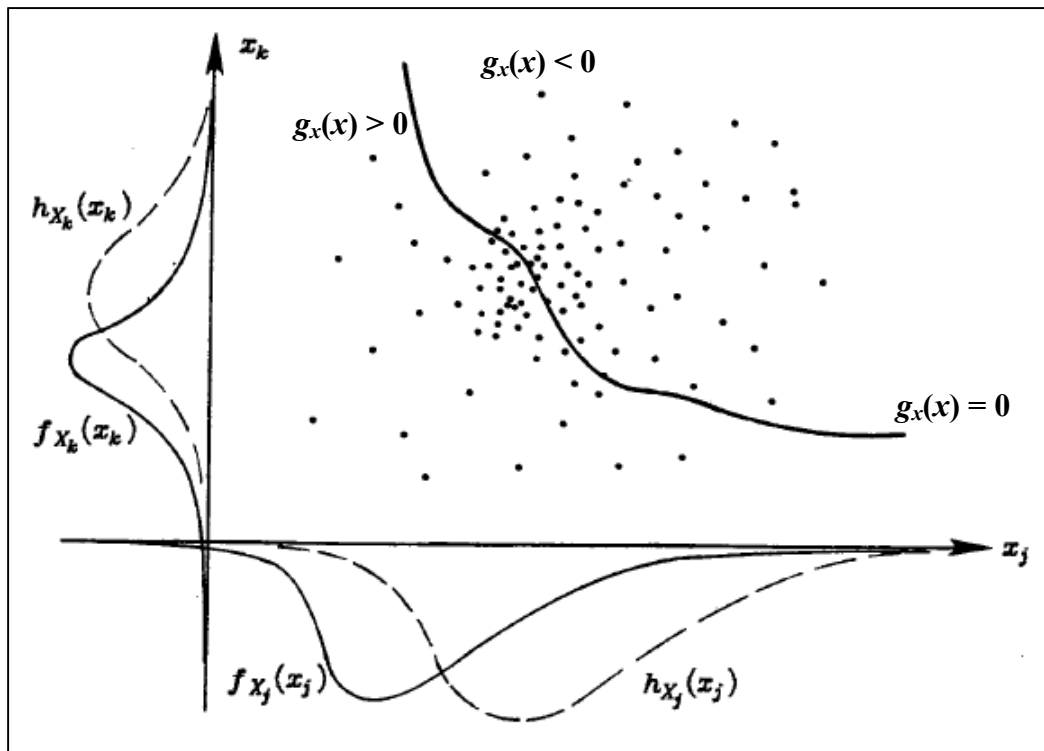
Figure 2.1 Comparison of typical outcomes using actual distribution $f_x(x)$ and IS sampling distribution $h_x(x)$ (Karamchandani 1987)

Although IS uses the concept of locating the MPP using β-based techniques, the former method has an upper hand over the later since it avoids the linearization errors associated with the β-based techniques. This is because the p_f is calculated based on simulation rather than direct β assessment. However, if the MPP cannot be located accurately, IS suffers with a poor solution.

Stratified Sampling (SS) or Latin Hypercube Sampling (LHS)

In SS or LHS, the RV range is divided in to a set number of intervals, and one value per interval is sampled per simulation, but the sampled intervals are not repeated. This forces all the interval ranges to be represented in the simulation such that the extreme values are also guaranteed to be sampled with the expectation of producing more failures. Hence p_f can be calculated with fewer samples. The failure probability is then computed using the theorem of total probability as follows:

$$p_f = \sum_{j=1}^{m} [P(R_j) \frac{1}{N_j} \sum_{i=1}^{N_j} I_g(x_i)] \tag{2.8}$$

where:

$P(R_j)$ = probability of region (interval) R_j

N_j = number of simulation cycles performed in region R_j

I_g = indicator function

The following is the stepwise procedure explaining the SS method in detail:

1. For each RV (x_i) in the limit state function, divide the PDF into equal intervals, N. The sized of each interval is chosen in such a way that the probability of a value

falling in the interval is 1/N. These are the cumulative distribution function (CDF) values of the interval.

2. Choose one standard normal CDF per interval to generate a random number. For a large number of intervals, usually the interval midpoint is selected. Use a proper conversion process to convert the standard normal CDF to basic RV space of the desired distribution.

3. Repeat the above process for each RV, as per MCS.

4. Evaluate the limit state based on the RV values in step 3.

5. Repeat the entire process without repeating an interval for RV number assignment in step 2.

6. Continue until all of the intervals are exhausted. When all intervals are exhausted, the results can be treated as those found from MCS.

Markov Chain Monte Carlo (MCMC)

Further research and developments were made to increase the efficiency of the crude MCS method, one of them being the MCMC approach. MCMC is an algorithm that obtains samples following the target distribution by generating samples from arbitrary probability distributions, based on a Markov chain designed to converge to the target distribution. Since samples after a large number of Markov chain steps converge to a stationary distribution, these samples can be regarded as almost independent samples from the target distribution (Furuta et al. 2010).

A Markov chain is a stochastic process where we transition from one state to another state using a simple sequential procedure. The chain starts at some state $x^{(1)}$ and uses a transition function $p(x^{(t)}|x^{(t-1)})$, to determine the next state, $x^{(2)}$ conditional on the last state. Repeated iterations are conducted to create a sequence of states. Each such sequence of

states is called Markov Chain. The procedure of generating a sequence of T states from a

Markov Chain is the following:

1. Set $t = 1$
2. Generate an initial value u, and set $x^{(t)} = u$
3. Repeat

    $t = t + 1$

    Sample a new value u from the transition function $p(x^{(t)}|x^{(t-1)})$
    Set $x^{(t)} = u$
4. Continue until $t = T$

The local dependence of the Markov chain on its last state makes this chain

'Markov' or 'memoryless'. An important property of Markov Chain is that the starting

state of the chain no longer affects the state of the chain after a sufficiently long sequence

of transitions. At this point the chain is said to reach its *steady state* and the state reflects

samples from it *stationary distribution*. The goal of MCMC is to design a Markov chain

such that the stationary distribution of the chain is exactly the distribution that we are

interesting in sampling from. This is called the *target distribution*. In other words, we

would like the states sampled from some Markov chain to also be samples drawn from

the target distribution. The idea is to use a method for setting up the transition function

such that a convergence to the target distribution is achieved. Metropolis sampling,

Metropolis-Hastings and Gibbs sampling are a few of the methods used to achieve the

aforementioned goal.

Reliability Index-Based Techniques (β-based techniques)

The β-based methods are analytical approximation techniques which uses the concept of reliability index (β); a substitute or a surrogate measure of probability of failure p_f. These methods were developed by researchers in order to reduce the computational effort required by the simulation techniques to solve problems having low failure probability.

Hasofer and Lind (1974) were the first to conceptualize the reliability index as the shortest distance from the origin of reduced random variables (RVs in standard normal space) to the failure boundary. A schematic representation of this concept is given in figure 2.2 and the mathematical expression for β is as shown in equation 2.9.

$$\beta = \frac{\mu_R - \mu_Q}{\sqrt{\sigma_R^2 - \sigma_Q^2}} \tag{2.9}$$

where:

β = reliability index also measured as the inverse of coefficient of variation (COV) of the limit state function $g = R - Q$

μ_R & μ_Q = mean of resistance and load RVs

σ_R & σ_Q = standard deviations of resistance and load RVs
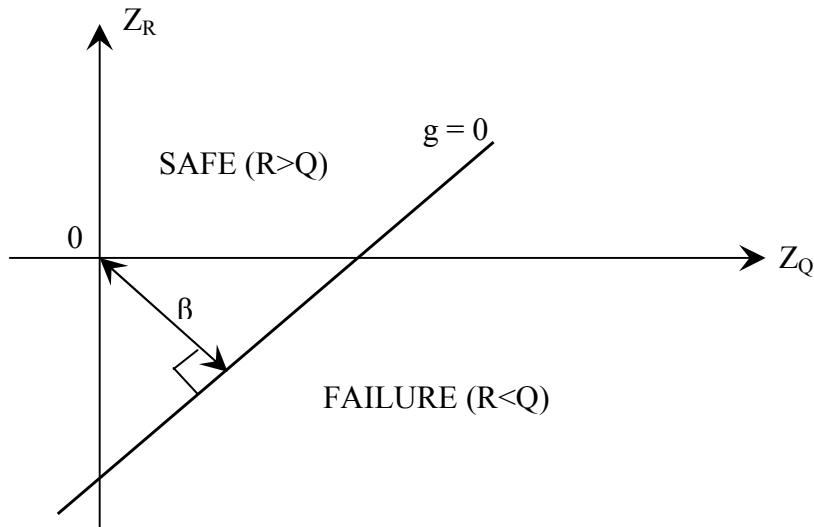
Figure 2.2: β defined as the shortest distance in the space of reduced RVs

For normally distributed RVs a relation between p_f and β can be established using a standard normal transformation as follows:

$$p_f = \Phi\,(-\beta) \tag{2.10}$$

First Order Reliability Method (FORM)

As described earlier, equation 2.9 is only limited to normal RVs. Hence, to account non-normal RVs, researchers suggested adjustments. Rackwitz and Fiessler (1978) proposed to transform the non-normal RVs to "equivalent normal" RVs at the design point. The transformation of a non-normal RV 'X' to a normal RV 'Y' is done is such that a standard normal distribution will result in the same probability (CDF value) at the design point.

Consider an independent non-normal RV X_i with mean (μ_x) and standard deviation (σ_x). Applying a first order expansion at the design point x^*, the CDF; $F_x(x)$ and PDF;

$f_x(x)$ of RV x can be described in terms of its equivalent normal mean μ_x^e and standard deviation σ_x^e as follows:

$$F_x(x^*) = \Phi(\frac{x^* - \mu_x^e}{\sigma_x^e})$$

(2.11)

$$f_x(x^*) = \frac{1}{\sigma_x^e}\phi(\frac{x^* - \mu_x^e}{\sigma_x^e})$$

(2.12)

Rearranging terms in equations 2.11 and 2.12 gives us the equivalent mean and standard deviation as follows:

$$\mu_x^e = x^* - \sigma_x^e[\Phi^{-1}(F_x(x^*))]$$

(2.13)

Where σ_x^e is given by following equation:

$$\sigma_x^e = \frac{1}{f_x(x^*)} \emptyset \left(\frac{x^* - \mu_x^e}{\sigma_x^e}\right)$$

$$= \frac{1}{f_x(x^*)} \phi[\Phi^{-1}(F_x(x^*))]$$

(2.14)

In case of dependent RVs, they must be transformed to equivalent independent RVs using the Rosenblatt transformation.

The Rackwitz-Fiessler algorithm for independent RVs is described as follows:

1. Develop a limit state function g for the problem.
2. Assume a trial design point. The design point is usually described in vector form $\{x_i^*\}$.
3. Compute equivalent normal means and standard deviations at the design point $\{x_i^*\}$ using equations 2.13 and 2.14, respectively.

4. Compute coordinates of the design point in normal space as given in equation 2.15:

$$\sigma_x^e = \frac{x_i^* - \mu_{Xi}^e}{\sigma_{Xi}^e} \qquad (2.15)$$

5. Compute the partial derivative of limit state in equivalent normal space

$$\frac{\partial g}{\partial x_i^e} = \frac{\partial g}{\partial x_i}\bigg|_{x_i^*} \sigma_{Xi}^e \qquad (2.16)$$

6. Compute new design point

$$\{Z_{i+1}^*\} = \left(\frac{1}{\sum_{i=1}^{n}\left(\frac{\partial g}{\partial x_i^e}\right)^2} \left[\sum_{i=1}^{n} \left(\frac{\partial g}{\partial x_i^e} \cdot Z_i^e \right) - g(X_i^e) \right] \cdot \left\{ \frac{\partial g}{\partial x_i^e} \right\} \right) \qquad (2.17)$$

7. Compute reliability index (β)

$$\beta = \sqrt{\sum_{i=1}^{n}(Z_{i+1}^*)^2} \qquad (2.18)$$

8. Compute updated design point in basic variable space

$$x_{i+1}^* = \mu_{Xi}^e + \sigma_{Xi}^e \cdot Z_{i+1}^* \qquad (2.19)$$

9. Repeat steps 3 to 8 until the solution converges to either of β or Z_i^* or $g = 0$.

Although computationally effective, FORM suffers with some drawbacks. For problems without linear limit states and all normal RVs, FORM produces approximate solutions only, which in some cases may be quite poor (Eamon et al. 2005, Charumas 2008, Haldar and Mahadevan 2000). These inaccuracies occur because the limit state is linearized and this approximation may not accurately represent the true failure boundary (Melchers 1999; Haldar and Mahadevan 2000). Secondly, although MCS is applicable to

any reliability problem, regardless of complexity, this is not true of β-based methods. In case of ill-behaved, discontinuous and highly non-linear limit states or limit states containing multiple 'local' MPPs, as in many problems requiring FEA solution, the MPP search algorithm may fail completely resulting in no solution (Haldar and Mahadevan 2000; Eamon and Charumas 2011).

Second Order Reliability Method (SORM)

As explained in the earlier section, the linear approximation of the limit state surface in FORM leads to a lack of accuracy for non-linear and non-normal limit state functions. The development of second moment methods was aimed to improve the non-linearity issue. The attempt has been to fit a parabolic, quadratic or higher order surface to the actual surface. The Second Order Reliability Method (SORM) is a method which approximates the limit state surface in standard normal space with a second order quadratic surface at the design point. A Taylor series expansion is usually used to achieve the approximation.

Breitung's (1984) version of SORM considers a parabolic approximation of the limit state surface and is a commonly followed second order reliability method. The following expression describes the probability of failure by SORM:

$$P_f = \phi(\beta_{FORM}) \prod_{i=1}^{n-1} (1 + \beta_{FORM} \cdot K_t)^{-1/2} \tag{2.20}$$

Here, the FORM result is used in the SORM failure probability calculation (Mitteau 1996). K_t is a Hessian of the limit state function expressed in matrix form. However, as seen in the expression above, the accuracy of SORM is highly dependent on the accuracy of FORM (β_{FORM}) to locate the MPP, which may result in an inaccurate

SORM solution if the MPP is not accurate itself or if the limit state boundary does not closely follow a parabolic shape.

Response Surface Method (RS) or Surrogate Modeling

Response surface techniques represent a class of optimization methodologies that make use of surrogate modeling techniques to quickly find the local or global optima. Surrogate modeling techniques are of particular interest for engineering design when high-fidelity thus expensive analysis codes are used. These techniques are often termed 'metamodeling techniques' .

Surrogate modeling techniques aim at regression and/or interpolation fitting of the response data at the specified training (observation) points that are selected using one of many designs of experiments (DOE) techniques. These training/observation points are chosen in such a way that their contribution towards failure probability is most important. The basic idea consists of using approximate simple functions at these training points and substitute the real limit state function with a response surface which is usually expressed in a simple form or represented by an explicit expression, and results in a reduction in computational costs (Gomes and Awruch, 2004).

To develop the approximate functions and the fitting procedure, several response surface techniques such as polynomial response surface (PRS) approximations, multivariate adaptive regression splines, radial basis functions (RBF), Kriging, Gaussian process and neural networks (Acar and Rais-Rohani, 2009) have been implemented. Fang et al (2005) found that RBF gives accurate metamodels for highly non-linear responses whereas Simpson et al. (2001) found Kriging best for slightly non-linear responses in

high-dimensional space. Jin et al. (2001) suggested the use of PRS for slightly non-linear and noisy responses.

From the aforementioned studies it can be noted that a particular technique was found to be suitable only for specific type of problem. Due to insufficient information related to the relationship between the response and the input variables, it is extremely difficult to predict which metamodel is best for a specific response. Goel et al. (2007) further pointed out the uncertainties in the metamodel predictions due to its dependency on selected DOE type, the number of design points in the training data set and the form of response. Hence, Acar and Rais-Rohani (2009) suggested an alternative approach of using an ensemble of metamodels in a weighted-sum formulation. The resulting hybrid metamodel takes the advantage of the prediction ability of each individual stand-alone metamodel to enhance the accuracy of the response predictions.

CHAPTER 3 ADVANCED FAILURE SAMPLING METHOD

Introduction to Advanced Failure Sampling Method

As explained in the previous sections of the thesis report the accurate application of β-based reliability analysis techniques is limited to well-behaved limit state functions. For many highly complex, non-linear and ill-behaved limit states the β-based methods either produce approximate solutions or fail to produce any results. On the other hand, the application of available simulation based methods such as MCS to solve the aforementioned limit state functions often requires high computational effort. As an alternative solution approach to complex reliability problems, this research proposes the Failure Sampling (FS) approach.

In general, the method uses conditional expectation to sample the complex (generally resistance) portion of the limit state function and estimate either its probability density function (PDF) or cumulative distribution function (CDF). Additional data needed for solution of high reliability problems can then generated by extrapolation, where the original sample may be fit to a flexible, multi-parameter curve to extend the tail region. Clearly, the accuracy of this approach is a function of how well the PDF or CDF estimate and resulting curve fit are developed. The following section describes the concept of the FS method along with its potential advantages over currently available reliability analysis techniques.

Summary of Advanced Failure Sampling Method

As explained in Chapter I, the probability of failure p_f of a limit state function g can be calculated by estimating a single-dimensional PDF of g and integrating the PDF over the failure region (i.e. where $g < 0$). Direct MCS can be used to generate the sample of g used to develop the PDF. Of course, this approach will yield accurate results only when the PDF of g can be estimated accurately. However, for typical structural reliability problems, the large majority of the sample generated from MCS is far from the failure region, resulting in a problem for which it is difficult if not impossible to accurately integrate the failure region without a high number of simulations.

In the FS approach, the initial limit state function $g(X_i)$, consisting of random variables X_i, is reformulated to a new limit state g^*. g^* is expressed in terms of a control random variable q, separated from the remaining random variables (RVs) $R(X_j)$. Setting g^* to zero to represent the failure condition, the problem can be written as:

$$g^* = R(X_j) - q = 0 \tag{3.1}$$

Where $R(X_j)$ may be regarded as the "resistance" of g^* while q is a "load" RV. Here g^* is mathematically equivalent to original limit state function g. Best results are usually obtained by selecting the RV with highest variation as the control variable, as its variation is then eliminated from subsequent simulation. However, there is no theoretical limitation in this regard, and q does not need to actually represent a load RV in the physical problem. However, q should be statistically independent of the remaining RVs X_j, as the current approach does not explicitly address the case where q is dependent with one or more of the remaining RVs, and solving such a problem with FS may introduce

error.   However, nearly all realistic reliability problems have at least some RVs that are independent; for example, in structural engineering, load and resistance RVs are practically always independent Once equation 3.1 is formed, values for X_j are simulated by a method such as MCS.   Note these initial steps are shared with the conditional expectation (CE) method, which is fully described elsewhere (Ayyub and Chia 1992; Ayyub and Haldar 1984).   However, at this point, FS differs from CE.   Here, it can be seen from equation. 3.1 that for a particular set of simulated values $R(x_j)$, $q = R(x_j)$.   That is, if a value of q can be determined to satisfy equation 2.20 that value also equals a datum for the sample of resistance $R(x_j)$. Note for complex problems, this generally requires a non-linear solver to determine q.   A value for q is thus determined for each set of simulated values $R(x_j)$, thereby developing an equivalent, single-dimensional data sample for the potentially very complex, multi-variate $R(x_j)$. Once the data sample for $R(x_j)$ is generated, there is no need to evaluate the true response further (e.g. no need for further finite element analyses, if that is how the limit state function is evaluated), and the bulk of the computational effort for a complex problem ends.   Next, depending on the solution approach, a PDF or CDF estimate of $R(X_j)$ is developed, rather than directly using the data sample of $R(X_j)$ to compute p_f of g^*. This additional step was found to significantly reduce variance in the solution.   Once the PDF or CDF estimate is formed, p_f of g^* (and thus of the original limit state function $g(X_i)$) can be found with a variety of methods, from direct integration over the region g<0 to curve-fitting approaches to represent the sample of $R(x_j)$ with an analytical distribution. If the latter approach is used, p_f can be computed very quickly with any method, such as MCS, for example, as the

original, potentially complex function $g*$ is now represented analytically (Eamon and Charumas 2011).

Step-by-Step Procedure For Advanced Failure Sampling Method

1. Choose a control RV, q, and reformulate g to $g*$ as shown in equation 3.1.

2. Simulate values for the RVs in $R(X_j)$ using a method such as Monte Carlo Simulation.

3. Once a set of MCS samples is generated, the value of control RV q is then incremented up or down until $g* = 0$. Root finding algorithms such as the Newton Raphson or Bisection techniques may be used to find roots for non-linear limit state functions.

4. A sufficient number of simulations are conducted by repeating steps 2 and 3.

5. A PDF of the resistance sample is estimated, or a known distribution is fit to the resistance points directly, to represent the data with an analytical PDF or CDF. The latter approach has the advantage of extending the tail of the distribution beyond that available from the original sample.

6. Once a PDF of $R(x_j)$ is estimated or a curve is fit to the resistance samples, the problem is reduced to a 2 RV equivalent form per. Equation 3.1, where any preferred reliability method can be used to calculate p_f with very low computational effort. These methods are discussed in detail in chapter three of this report.

Advantages and Limitations of Advanced Failure Sampling Method

In summary, the FS approach offers the following advantages:

1. As there is no reliance on the MPP, complex problems for which the MPP cannot be located, and thus which are unsolvable by methods such as FORM, SORM, and importance sampling approaches, can be addressed.

2. For many complex, moderate reliability (i.e. reliability index from 3-5) problems that are poorly solved or unapproachable with many other methods, computational effort is low, often on the order of 1000 simulations, for reasonably accurate solutions.

3. The method is mathematically simple and straightforward to implement.

Some important limitations to the method are:

1. The control variable q should be independent of the remaining RVs. As noted earlier, for almost all practical structural reliability problems, some RVs are uncorrelated, so this criteria is readily met. However, solution accuracy may be reduced if a correlated RV is indeed considered for q.

2. A nonlinear root finder is typically required. The efficiency of the root finder will affect the efficiency of the solution, as this effects how many calls are required to the finite element code to evaluate the true response of $R(x_j)$.

3. Although theoretically unlimited, some choices of q may be practically limited by the physical nature of the problem. That is, a q could be chosen that requires values to set $g^*=0$ that are beyond the realm of physical possibility for a particular problem.

4. The method is intended for complex problems for which reliability-index based methods provide no or poor solutions, and for which other simulation methods require an infeasibly large computational effort. For other problem types, other methods are generally more efficient.

Development of Enhanced Advanced Failure Sampling Method

Development of Optimal Algorithm for PDF Construction

Construction of the PDF estimate of resistance samples $R(x_j)$ is a critical step in the FS process, as the pf estimate directly depends on $R(x_j)$. Therefore, several alternative methods were investigated to determine accuracy and efficiency. These are the interval method, the curve-fit method and the design optimization method. The details of these approaches are given in the following sub-sections.

Interval Method

This method was proposed in the original implementation of FS (Eamon and Charumas 2011). In this approach, a raw PDF of system resistance is developed. Once the PDF estimate is obtained, the most straightforward way to calculate p_f is by numerical integration (NI) of the well-known expression:

$$p_f = \int_{-\infty}^{\infty} F_R(x) f_q(x) dx \tag{3.2}$$

In equation 3.2, $F_R(x)$ refers to the estimated CDF of $R(x_j)$. It is obtained directly from the estimated PDF by numerical integration of:

$$F_R(x) = \int_{-\infty}^{x} f_q(x) dx \tag{3.3}$$

Note this is not the CDF of the original data sample found in steps 3 and 4 of the algorithm above, but the CDF of the PDF estimate, which generally contains many fewer points. The PDF is usually constructed by dividing the data into equally spaced intervals, counting the number of data in each interval, then normalizing the values such that the PDF has a total area of 1.0. For instance, assume the PDF was estimated by dividing 1000 resistance data into 50 intervals. A 50-point CDF estimate is then obtained by numerically integrating the PDF using equation 3.3. For FS, it was reported that an interval size of 50 for a resistance sample size of 1000 has generally resulted in accurate solutions. However, this selection was somewhat arbitrary, and changing the interval size affects the PDF and thus the accuracy of the solution.

Moreover, the interval size may be subject to change as the size of the resistance sample $R(x_j)$ is increased or decreased. Although not directly related to FS, some guidance is available in the literature for selecting an interval size relative to sample size in general. For example, an estimate given by Ayyub and McCuen (2003) is:

$$i = 1 + 3.3\log(n) \tag{3.4}$$

where:

i = number of intervals

n = number of data

However, empirical approaches such as those described in equation 3.4 are not effective in many cases. Using the above expression, for a resistance sample size of 1000, the required interval size is 11, which was found to poorly work in the case of FS, where

an interval size of 50 was observed to have most accurate results for 1000 data. Hence, this research aims to determine the optimum interval size for the FS method.

Curve-Fit Method

Rather than using NI, an analytical distribution can be fit to the resistance samples. This alternative approach is considered with an objective to by-pass the difficulty of determining the interval size. The advantage of fitting an analytical distribution to the data is twofold;

1. Since an analytical distribution provides a continuous function, the tail of the distribution can be extended beyond that available from the original sample. This helps in capturing the lower range values of resistance data needed to calculate very low p_f. On the other hand, with the interval approach, the lower range value of resistance is limited to the value captured in the last discrete interval.

2. If the resistance sample is fit to an analytical curve, probability of failure can be calculated quickly using any reliability method such as MCS, FORM etc. with no need for numerical integration.

Generalized Lambda Distribution (GLD)

The Generalized Lambda Distribution (GLD) is a four parameter distribution that can be applied to various reliability analysis problems and is known for its high flexibility. It can accurately fit many of the common statistical distributions such as Normal, Lognormal, Weibull, and others (Karian and Dudewicz 2010). The GLD is defined by it four parameters λ_1, λ_2, λ_3 and λ_4. The parameters λ_1 and λ_2 are location and

scale parameters, respectively, while λ_3 and λ_4 represent skewness and kurtosis. The estimation of the GLD parameters is not straightforward as this process has no closed-form solution, as discussed below. In this study, the method of moments has been used to estimate the parameters of the GLD. In the method of moments, the first four central moments of the GLD; the mean, variance, skewness and kurtosis, are matched with the sample moments about the mean value. The first four central moments of GLD are given as follows (Karian and Dudewicz 2010):

$$\mu = \lambda_1 + A / \lambda_2 \tag{3.5}$$

$$\sigma^2 = (B - A^2) / \lambda_2^2 \tag{3.6}$$

$$\mu_3 = (C - 3AB + 2A^3) / \lambda_2^3 \tag{3.7}$$

$$\mu_4 = (D - 4AC + 6A^2B - 3A^4) / \lambda_2^4 \tag{3.8}$$

where:

$$A = \frac{1}{(1 + \lambda 3)} - \frac{1}{(1 + \lambda 4)} \tag{3.9}$$

$$B = \frac{1}{(1 + 2\lambda 3)} - \frac{1}{(1 + 2\lambda 4)} - 2\beta(1 + \lambda_3, 1 + \lambda_4) \tag{3.10}$$

$$C = \frac{1}{(1 + 3\lambda 3)} - \frac{1}{(1 + 3\lambda 4)} - 3\beta(1+2\ \lambda_3,\ 1+\ \lambda_4) + 3\beta(1+\ \lambda_3,\ 1+2\ \lambda_4) \qquad (3.11)$$

$$D = \frac{1}{(1 + 4\lambda 3)} - \frac{1}{(1 + 4\lambda 4)} - 4\beta(1+3\ \lambda_3,\ 1+\ \lambda_4) + 6\beta(1+2\ \lambda_3,\ 1+2\ \lambda_4) \qquad (3.12)$$

$$- 4\beta(1+\ \lambda_3,\ 1+3\ \lambda_4)$$

In the above equations, β represents the beta function.

To fit the GLD to the resistance sample data, the GLD moments are equated to the first four sample moments about the mean in order to obtain the estimated moments of the GLD. Sample coefficients of skewness and kurtosis are obtained as follows:

$$\alpha^*_3 = m_3\ /\ (m_2)^{3/2} \qquad (3.13)$$

$$\alpha^*_4 = m_4\ /\ (m_2)^2 \qquad (3.14)$$

where m_2, m_3 and m_4 are the second, third and fourth sample moments about the mean respectively. Then, λ_3 and λ_4 can be obtained by solving the following two simultaneous equations:

$$\alpha^*_3 = \alpha_3\ (\lambda_3,\ \lambda_4) \qquad (3.15)$$

$$\alpha^*_4 = \alpha_4\ (\lambda_3,\ \lambda_4) \qquad (3.16)$$

where α_3 and α_4 are the coefficients of skewness and kurtosis of the GLD, given as:

$$\alpha_3 = \mu_3 / \sigma^3 \tag{3.17}$$

$$\alpha_4 = \mu_4 / \sigma^4 \tag{3.18}$$

The solutions for the above simultaneous equations can be found by using a Sequential Quadratic Programming (SQP) optimization scheme and minimizing the constrained function. The objective function is:

$$\min: f(\lambda,\lambda) = \{\alpha^*_3 - \alpha_3(\lambda_3,\lambda_4)\}^2 + \{\alpha^*_4 - \alpha_4(\lambda_3,\lambda_4)\}^2 \tag{3.19}$$

The above equation is subjected to the constraint: $\lambda_3\lambda_4 > -1/4$. The outcome of the minimization produces λ_3 and λ_4. The remaining parameters λ_1 and λ_2 can then be obtained from:

$$\lambda_2 = \pm[(B - A^2)/m_2]^{1/2} \tag{3.20}$$

$$\lambda_1 = m_1 - A/\lambda_2 \tag{3.21}$$

In this subtask, the GLD is used with MCS to calculate the probability of failure. Hence for generating the resistance samples, the following percentile function is used:

$$Y = \lambda_1 + [u^{\lambda_3} - (1 - u)^{\lambda_4}]/\lambda_2; \quad \text{where } 0 \le u \le 1 \tag{3.22}$$

The important criteria to achieve good results with the GLD is to maintain the smallest possible difference between α^*_3 and α_3 as well as α^*_4 and α_4. Appendix C presents the results for the GLD approach for various limit states considered.

Extended Generalized Lambda Distribution (EGLD)

Using the GLD, the (α^2_3, α_4) space is confined within the relationship: $1.8(\alpha^{*2}_3 + 1) < \alpha^*_4 < 1.8\,\alpha^{*2}_3 + 15$, potentially limiting the GLD's effectiveness on some limit states. The upper restriction on α^*_4 may be overcome with additional computational effort. However, the lower restriction is imposed to prevent numerical difficulties with the solution. To address the lower limit problem (i.e. for $\alpha^*_4 < 1.8(\alpha^{*2}_3 + 1)$), another curve fit approach using the Extended Generalized Lambda Distribution (EGLD) method is explored. Figure 1. shows the (α^2_3, α_4) space covered by GLD & EGLD.

The EGLD method addresses the limitation of the GLD method to provide curve fits in the region $1 + \alpha^{*2}_3 < \alpha^*_4 < 1.8(\alpha^{*2}_3 + 1)$. The EGLD is defined by its four parameters β_1, β_2, β_3 and β_4. Unlike the GLD, the EGLD is defined by its PDF and is given as follows (Dudewicz and Karian 1996):

$$f(x) = \frac{(x - \beta_1)^{\beta_3}(\beta_1 + \beta_2 - x)^{\beta_4}}{\beta(\beta_3 + 1, \beta_4 + 1)\beta_2^{(\beta_3 + \beta_4 + 1)}} \tag{3.23}$$

where $\beta_1 < x < \beta_1 + \beta_2$

Similar to the GLD, the unknown parameters of EGLD are determined using the method of moments. The mean, variance, skewness and kurtosis of EGLD are defined as follows:

$$\alpha_1 = \beta_1 + \frac{\beta_2\ (\beta_3 + 1)}{B_2} \tag{3.24}$$

$$\alpha_2 = \frac{\beta_2^2(\beta_3+1)(\beta_4+1)}{B_2^2 B_3} \tag{3.25}$$

$$\alpha_3 = \frac{2(\beta_4-\beta_3)\sqrt{B_3}}{B_4\sqrt{(\beta_3+1)(\beta_4+1)}} \tag{3.26}$$

$$\alpha_4 = \frac{3B_3(B_2\beta_3\beta_4+3\beta_3^2+5\beta_3+3\beta_4^2+5\beta_4+4)}{B_4 B_5(\beta_3+1)(\beta_4+1)} \tag{3.27}$$

where $B_i = \beta_3 + \beta_4 + i$.

It can be observed from the above equations that the skewness and kurtosis of EGLD are defined in terms of β_3 and β_4 only. Hence, by equating the sample skewness and kurtosis with that of the EGLD leads us to two simultaneous equations as follows:

$$\alpha^*_3 = \alpha_3 (\beta_3, \beta_4) \tag{3.28}$$

$$\alpha^*_4 = \alpha_4 (\beta_3, \beta_4) \tag{3.29}$$

β_3 and β_4 values can then be determined by using a SQP optimization method applied to the following minimization function:

$$\min: f(\lambda,\lambda) = \{\alpha^*_3 - \alpha_3 (\beta_3, \beta_4)\}^2 + \{\alpha^*_4 - \alpha_4 (\beta_3, \beta_4)\}^2 \tag{3.30}$$

Unlike the GLD, the EGLD minimization function is not a constrained function; i.e. the β_3 and β_4 values are unconstrained. Once the β_3 and β_4 values are determined, the β_1 and β_2 values can be obtained as follows:

$$\beta_2 = (\beta_3 + \beta_4 + 2)\sqrt{\frac{(\beta_3+\beta_4+3)\alpha_2^*}{(\beta_3+1)(\beta_4+1)}} \tag{3.31}$$

$$\beta_1 = \alpha_1^* - \sqrt{\frac{\beta_2(\beta_3+1)}{(\beta_3+\beta_4+2)}} \tag{3.32}$$

Once the unknown parameters of the EGLD system are determined, the EGLD random variables can be generated using the following relation:

$$Y = \beta_1 + \beta_2 X \tag{3.33}$$

Here Y is a EGLD random variable with parameters β_1, β_2, β_3 and β_4 and X is a beta random variable with parameters β_3 and β_4. These generated values of EGLD are then used with MCS to determine the probability of failure or the reliability index (β).
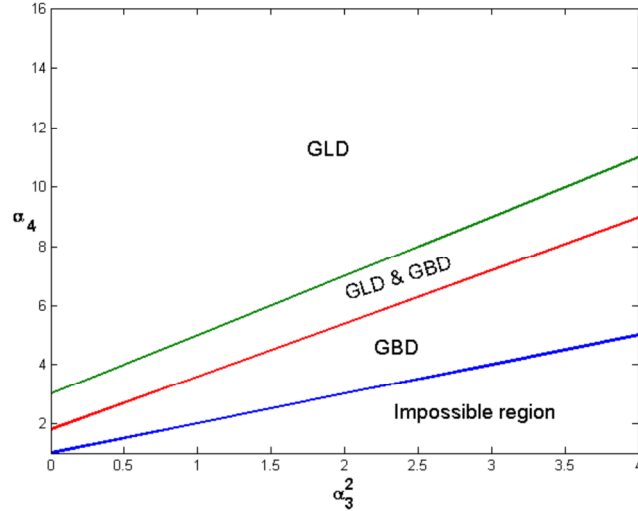
Figure 3.1. ($\alpha 23$, $\alpha 4$) Space Covered by the GLD and EGLD (GBD) (Acar *et al.* 2008).

Johnsons Distribution (JSD)

The Johnson's system of distribution consists of a family of distributions and has the flexibility of covering a wide variety of shapes. JSD is based on three possible transformations of a normal random variable, plus an identity transformation. The 'SB' transformation represents a bounded JSD, the 'SL' transformation represents a semi-bounded JSD, and the 'SU' transformation represents the unbounded JSD. The SB, SL and SU transformation can be represented as follows:

$$X = \gamma + \delta \cdot \Gamma\left(\frac{z - \xi}{\lambda_j}\right) \tag{3.34}$$

where Z is a standard normal random variable; Γ denotes the transformation function; γ and δ are shape parameters; ξ is the location parameter; and λ_j is the scale parameter. The 'SN' transformation is the identity transformation and represents a normal Johnson distribution. Although various methods to determine the parameters of JSD are available, the method of moments, method of percentiles, and method of quantile estimators are most popular. In this research, the method of quantile estimators was used to determine the parameters. If X follows a Johnsons distribution and $Y = \frac{X-\xi}{\lambda}$, then the PDFs of the respective transformations can be described as follows:

SB Family:

$$p(y) = \frac{\delta}{\sqrt{2\pi}} \times \frac{1}{[^y/_{(1-y)}]} \times \exp\left\{-\frac{1}{2}\left[\gamma + \delta.\ln\left(\frac{y}{1-y}\right)\right]^2\right\} \tag{3.35}$$

SL Family:

$$p(y) = \frac{\delta}{\sqrt{2\pi}} \times \frac{1}{[y]} \times \exp\left\{-\frac{1}{2}[\gamma + \delta.\ln(y)]^2\right\} \tag{3.36}$$

SU Family:

$$p(y) = \frac{\delta}{\sqrt{2\pi}} \times \frac{1}{[\sqrt{y^2+1}]} \times \exp\left\{-\frac{1}{2}\left[\gamma + \delta.\ln\left(y + \sqrt{y^2 + 1}\right)\right]^2\right\} \tag{3.37}$$

Once the parameters and the type of JSD family is determined, a resistance sample is generated using the inverse function given by eq. 3.38. At this point, the limit state is completely analytically defined and any reliability method can be used to estimate failure probabilty with minimal computational effort. In this task, MCS was used to calculate the probability of failure.

$$X = \xi + f^{-1}\left(\frac{z-\gamma}{\delta}\right) \tag{3.38}$$

Generalized Extreme Variation Distribution (GEV)

The GEV distribution combines three simpler distributions into a single form, allowing a continuous range of possible shapes that includes the three component distributions. Similar to the extreme value distribution, the GEV is often used to model the smallest or largest values among a large set of independent, identically distributed random values. It is a three parameter distribution defined by a location parameter μ, a scale parameter σ, and a shape parameter k; where k must take a value other than zero. The PDF of the GEV is given as:

$$y = \frac{1}{\sigma}\exp\left(-\left(1+k\frac{(x-\mu)}{\sigma}\right)^{\frac{-1}{k}}\right)\left(\left(1+k\frac{(x-\mu)}{\sigma}\right)^{-1-\frac{1}{k}}\right) \tag{3.39}$$

The parameters of the GEV distribution were determined using standard library functions given in Matlab (2012b).

Design Optimization Method

The numerical integration method and the curve fit methods have their own limitations in yielding good results for all types of structural reliability problems. Further, it was observed that each of the curve fit methods explained earlier may only work for certain types of problems. In order to obtain consistently superior results, a hybrid method that uses a technique from design optimization to combine the features of the interval method as well as each of the curve-fit approaches for optimal PDF construction is studied in this research. The aim of this task is to develop a consistent method to form

the PDF such that the failure probability is estimated with maximum accuracy and minimum variance for any problem type. The mechanism that will be used to combine these PDFs is an optimized ensemble technique (Acar and Rais-Rohani 2009).

The optimized ensemble technique was originally developed for response surface construction. The purpose of the response surface is to save computational effort for repetitive analyses by representing a complex response function, such as that found from FEA, with a surrogate analytical function, or a metamodel, which is 'fit' to the true response. It is known that certain metamodels best fit certain response characteristics. For example, Fang et al. (2005) and Rais-Rohani, et al. (2006) found that radial basis functions give accurate metamodels for highly nonlinear responses; Simpson et al. (2001) found Kriging to be most suitable for slightly nonlinear responses in high dimension spaces; and Jin et al. (2001) found polynomial surfaces work well for noisy responses. However, complex responses are often characterized in multiple ways; for example, a response that is both highly nonlinear as well as noisy. For these cases, it would be desirable to take advantage of the predictive capability of various metamodelling approaches. Therefore, in the ensemble approach, not one, but multiple metamodels are constructed for a problem (Bishop 1995; Zerpa et al. 2005; Goel et al. 2007; Acar and Rais-Rohani 2008). Here, a unique ensemble of metamodels is developed for a specific problem by representing the final metamodel as a weighted sum of two or more stand-alone metamodels, each separately fitted to the same response. The resulting hybrid metamodel takes advantage of the prediction ability of each individual stand-alone metamodel to enhance the accuracy of response predictions. Generally, the weight factors

were chosen based on trial and error or engineering judgment (Goel et al. 2007). However, with the optimized ensemble approach, the weight factors are chosen based on design optimization. This was found to provide results of greatest consistency and accuracy (Acar and Rais Rohani 2009). In this research, the optimized ensemble technique is extended beyond response surface development and used for optimum PDF construction for FS. The concept is to form an ensemble of all the PDFs generated by NI as well as various curve-fit methods. The ensemble is constructed in such a way that all the stand-alone PDFs obtained from NI, JSD, GLD, GEV, and any other curve fit or PDF construction method desired, are assigned weight factors depending upon their individual accuracy. Using a weighted sum formulation, an ensemble of PDFs is thus formulated as follows:

$$f_{RE}(x) = \sum_{i=1}^{N} w_i(x) f_i(x) \qquad (3.40)$$

Where f_{RE} is the final ensemble PDF developed from N stand-alone PDFs $f_i(x)$. In the current research; four stand-alone PDFs, each obtained from NI, JSD, GEV and GLD were considered. $W_i(x)$ is the weight factor of ith stand-alone PDF and x is the vector of independent input variables. The weight factors are subjected to following constraint.

$$\sum_{i=1}^{N} w_i(x) = 1 \qquad (3.41)$$

The weight factors are determined by an optimization process where the difference between the true PDF and the stand-alone PDFs is minimized. For this

research, the Sequential Quadratic Programming (SQP) optimization technique is used. Although the development of a "true" PDF for minimization is impossible, as PDF construction depends on the interval size used, a true CDF of x input variables is available and can be expressed as follows:

$$F_R(x_i) = \frac{s}{1+n} \tag{3.42}$$

where $F_R(x_i)$ is the CDF value for datum s. Hence, the above given equation (3.40) can be written in terms of CDF as:

$$F_{RE}(x) = \sum_{i=1}^{N} w_i(x)F_i(x) \tag{3.43}$$

where F_{RE} is the final ensemble CDF of N stand-alone CDFs $F_i(x)$. Here the error metric between the true CDF and ensemble CDF is measured using the generalized mean square error (GMSE) and is given as:

$$GMSE = \frac{1}{N} \sum_{k=1}^{N} (y^k - y_i^k)^2 \tag{3.44}$$

where y_k is the true CDF and y_i^k are the ensemble CDF values. Hence the final optimization problem has the following form:

$$\min \varepsilon_e = Err\{F_{RE}\left(w_i, y_i^k(x^k)\right)y(x^k), k = 1 \in N \quad s.t. \quad \sum_{i=1}^{N} w_i(x) = 1 \tag{3.45}$$

where $Err\{\}$ is the GMSE error metric and measures the accuracy of the ensemble CDF.

A MATLAB program was developed for the ensemble optimization process described above. The distribution functions obtained from GLD, JSD and GEV were considered to

form an ensemble. The ensemble was formed by solving equation (3.45) using *fmincon*, a function optimizer of MATLAB. The lower bound of the optimzer was specified as zero whereas the upper bound was set to one. The weights obtained for respective curves were then used to determine the probability of failure using traditioanl MCS as follows:

1. Fit each curve (GLD, JSD and GEV) to the resistance $R(x_j)$ data.

2. Determine the weight factors for each curve-fit method using the ensemble technique described above.

3. Generate a uniform RV, and using the appropriate curve parameters and coefficients, transform the uniform RV into three different basic random values (one each for GLD, JSD, and GEV) to represent resistance 'R'.

4. Multiply each random value of 'R' obtained in step 3, with the respective weights obtained from step 2.

5. Sum the weighted 'R' values from step 4 to obtain a single RV value for resistance 'R'. Note that this RV is now a hybrid value that represents some combination of the different distributions considered.

6. Repeat steps 2 -5 to generate additional resistance data as needed; this was typically limited to a sample size of 1000.

Efficient Method to Generate $R(X_i)$ Samples

MCS is a non-MPP (most probable point of failure) based simulation technique and is an integral part of the FS process. MCS was used to generate the raw resistance sample in the preliminary steps of FS, as well as for calculating the probability of failure when FS was coupled with the curve-fit techniques (See Appendix A). However, the use

of MCS within FS represents the most computationally expensive option. Some significant reductions in computational effort can be achieved with the use of variance reduction techniques such as stratified and importance sampling. However, these techniques are often associated with difficulties or inefficiencies for some types of complex problems (Eamon and Charumas 2011; Eamon et al. 2005). In particular, methods which rely on identifying MPP such as importance sampling may fail to provide any solution for a complex reliability problem, and thus re-introduce the very problem that FS was formulated to solve. Hence, an alternative non-MPP based simulation approach, the Markov Chain Monte Carlo (MCMC) Method, was considered for integration with FS for resistance sample generation. The objective was to further enhance the computational efficiency of the FS method. A description of MCMC and its integration with FS is described below.

Markov Chain Monte Carlo (MCMC)

MCMC is "memory-less" process that generates dependent samples that have the same limiting distribution as that of the RV of interest. The process ensures to cover the entire reliability space as sampling is conducted from all parts of the distribution including the tail regions (Steyvers 2011). This improves the efficiency and the accuracy of the simulation process.

A Markov chain is a sequential procedure where the next realized value of a RV depends only on the previous realized value; that is, a sequence of RV values x_0 , x_1 … is generated such that a value in the chain x_{t+1} is a function of the previous value in the chain x_t, where $t > 0$. Here x is the specific realization of a RV (state) at iteration 't'. The

process starts with generating an initial value 'u' for the RV, also referred as the starting

state $x_{(t)}$. The next RV realization $x_{(t+1)}$ in the sequence is generated using a transition

function or transition kernel; $p(x_{(t)}|x_{(t-1)})$. The process is repeated to have a total of T

sequences. The local dependency of the next value on its previous value makes this chain

memory-less. Using this chain, samples are generated from an arbitrary distribution until

convergence is obtained to a target distribution (Furuta, Miyake and Tsukiyama 2010).

The following algorithm briefly describes the generation of a sequence from a Markov

chain (Steyvers 2011):

1. Set $t = 1$

2. Generate an initial value u, and set $x_{(t)} = u$

3. Repeat:

   $t = t + 1$

   Sample a new value u from the transition function $p(x_{(t)}|x_{(t-1)})$

   Set $x_{(t)} = u$

4. Continue until $t = T$

After a sufficient number of sequences of transitions, the state of the chain is no

longer dependent on the initial state and the Markov Chain is said to reach a steady state.

At this point the stochastic Markov Chain is said to be stationary and the samples of the

chain reflect the target distribution. The objective of MCMC is to achieve a stationary

distribution which is similar to the target distribution. Various sampling techniques such

as Metropolis-Hastings, Gibbs, Slice, as well as others, are methods that can be used to

allow convergence to the target distribution. Metropolis-Hastings sampling is considered in this research, as described below.

Metropolis Hastings Sampling

As mentioned above, the goal of MCMC is to achieve a stationary distribution which is similar to the target distribution; i.e. to sample the RVs from the Markov chain in such a way that the samples also represent the target distribution. Let the density of the target distribution be denoted as *p(x)* such that $-\infty < x < \infty$. Say the current state (RV value) of the chain is *x*. A new candidate point *y* is generated using the conditional probability density $q(y|x)$. This conditional probability density is referred to as the proposal distribution. The proposed new candidate point is either accepted or rejected using the following acceptance probability (α).

$$\alpha = \min\left(1, \frac{p(y)q(x|y)}{p(x)q(y|x))}\right) \tag{3.46}$$

The decision of acceptance or rejection is determined by generating a value *u* from a uniform distribution (Steyvers 2011). The proposal is accepted if $u \leq \alpha$ and the new candidate point becomes $y^t = y$. However, if $u \geq \alpha$, the proposal is rejected and the new candidate point remains the same as the old state, $y^t = y^{t-1}$. This procedure is repeated until a steady state is obtained. The procedure is as follows (beginning with $t = 0$):

1. Initialize the chain by generating an initial value *x*.

2. Generate a candidate point *y* from $q(y|x)$.

3. Generate u a uniform random variate.

4. Calculate the acceptance probability $\alpha = \min\left(1, \frac{p(y)q(x|y)}{p(x)q(y|x))}\right)$

5. If $u \leq \alpha$, accept the proposal and set $y^t = y$; otherwise set $y^t = y^{t-1}$.

6. Set $t = t + 1$ and repeat the process from steps 3 through 6.

CHAPTER 4 VALIDATION AND VERIFICATION

To evaluate the effectiveness of FS method, a database of test problems is assembled and solved considering the various alternative approaches discussed earlier in Chapter 3. In order to study the effectiveness of FS method and facilitate comparisons of accuracy and efficiency, these problems are solved with a selection of other applicable reliability techniques mentioned earlier in literature review. The database includes existing benchmark reliability problems as well as a series of more realistic, complex problems representative of engineering practice. Benchmark reliability problems found in the literature include those suggested by Engelund and Rackwitz (1993), Robinson and Atcitty (1999), Pandey and Sarkar (2002), Eamon et al (2005), and Au et al. (2007). These problems include: very highly nonlinear problems; problems with multiple reliability indices; series and parallel systems; and noisy limit states. Eamon et al (2005) suggested a matrix of 22 test problems that systematically altered important parameters including: limit state linearity, RV distribution type, RV COV, number of RVs, correlation, and target failure probability. These existing analytical problems are useful for comparison as they demand minimal computational effort and are easily replicated and verified by other researchers. Moreover, as analytical problem formulation is easily controlled by adjusting parameters, they can also be used to catch specific areas of concern (for example, if the reliability method has particular difficulty with correlation, or high COV problems). Any problems identified may require appropriate adjustment in the FS process.

Herein, FS is also validated on several practical engineering problems which are computationally complex and costly. The problems selected for the validation of FS were based on following three important characteristics:

1. Sufficient computational complexity representative of realistic computational mechanics problems in engineering practice.

2. Moderately low failure probability.

3. An unidentifiable MPP.

An important issue related to the aforementioned nature of problems is how to determine the exact solution for comparison to FS. In such cases direct simulation methods which are independent of MPP, are the only viable solution for determining the exact solution. Here failure probability must be limited to a reasonable lower level such that computational costs are feasible (much lower failure probabilities can be explored with problems that are analytically constructed, above).

This chapter is divided into two major category of problems. The first includes series of problems of numerical nature. These are the problems where the limit state function has an analytical expression. These include the benchmark analytical problems described above. The second category deals with realistic engineering problems requiring FEA code. These are practical engineering problems of complex nature with low failure probability and unidentifiable MPP.

Limit State Functions Considered for Numerical Problems

General Limit State Function

To evaluate the effectiveness of the methods used to implement FS and develop recommendations for the Advanced FS approach, various problems were considered for solution. The first series of these is represented by a matrix of general analytical limit state functions. Specific parametric variations included: number of random variables (RVs), where 2, 5, and 15 RVs were considered; RV variance, where each random variable case considered two different coefficients of variation, 5% and 35%; distribution type, where normal, lognormal and extreme Type I were considered; linearity, where linear, moderately nonlinear, and highly nonlinear limit states were considered; and target reliability index, where 'high' and 'low' values were considered. Here, reliability indices falling in the range of 2 - 5 were considered 'high', whereas indices between 0.3 - 2 were considered 'low'. These combinations resulted in a total of 96 different general limit state functions which were evaluated. These benchmark limit state functions are taken from Eamon et al (2005). Figure 4.1 describes a flow chart for developing the different cases of the general limit state function.

The general form of the limit state function under study was as follows:

$$g = k \sum_{i=1}^{n} d_i - c \sum_{j=1}^{k} \frac{L_j^4 w_j}{E_j I_j} \tag{4.1}$$

The above function describes the limit state function of a uniformly loaded beam in terms of its deflection. The general cases considered, in terms on number of RVs and linearity, are as follows, with RV values in **boldface:**
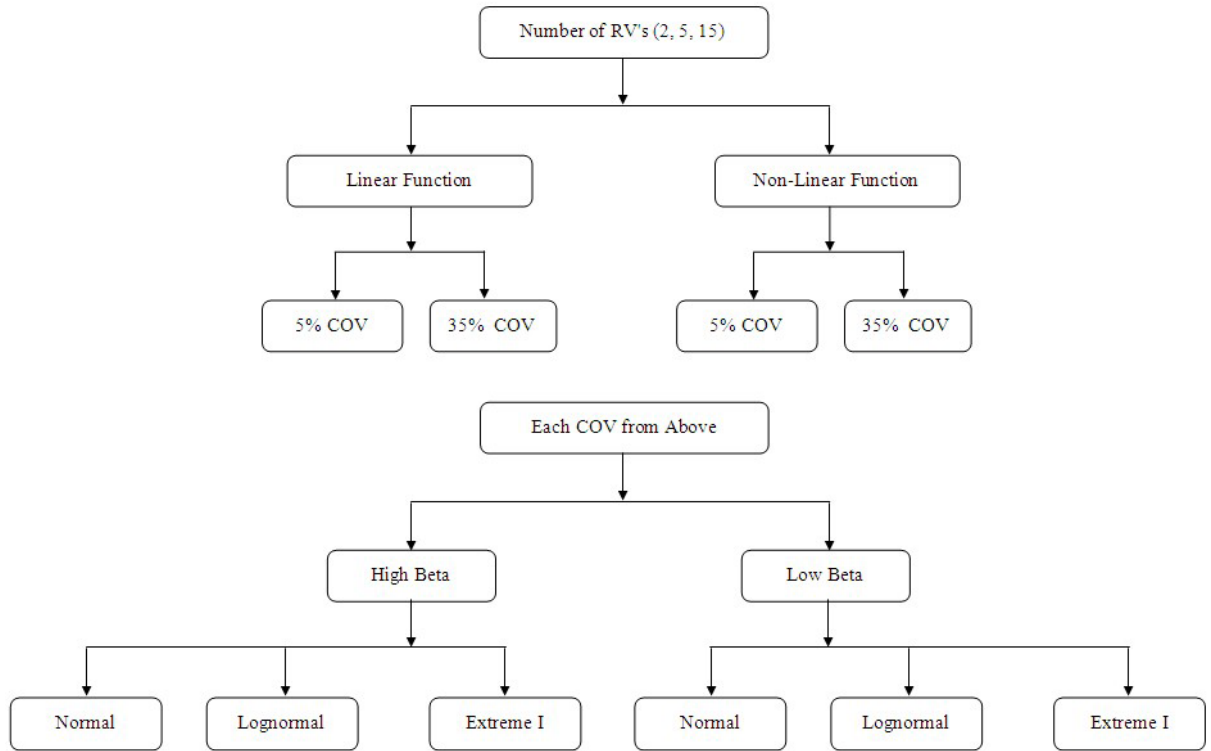
Figure 4.1. Flowchart for the General Limit State Functions

2 RV linear case

$$g = kd_1 - \frac{cL^4}{EI}w_1 \tag{4.2}$$

5 RV linear case

$$g = k(d_1 + d_2) - \frac{cL^4}{EI}(w_{DL1} + w_{LL1} + w_{LL2}) \tag{4.3}$$

15 RV linear case

$$g = k(d_1 + d_2 + d_3 + d_4 + d_5) - \frac{cL^4}{EI}(w_{DL1} + w_{LL1} + w_{DL2} + w_{LL2} + w_{DL3} +$$

$$w_{LL3} + w_{DL4} + w_{LL4} + w_{DL5} + w_{LL5}) \tag{4.4}$$

2 RV Non-linear case

$$g = kd_1 - \frac{cw}{EI}L^4 \tag{4.5}$$

5 RV non-linear case

$$g = kd_1 - c\frac{wL^4}{EI} \tag{4.6}$$

15 RV non-linear case:

$$g = k(d_1 + d_2 + d_3) - c\left(\frac{w_1L_1^4}{E_1I_1} + \frac{w_2L_2^4}{E_2I_2} + \frac{w_3L_3^4}{E_3I_3}\right) \tag{4.7}$$

The values in Table 4.1. have been used either as the mean value if a RV, or a constant value if a non-RV, of the parameter in question, depending on the case type:

Table 4.1. Parameters for General Limit State Functions

Parameter	Value
C	5/384
L	6.1 (m)
E	2 x 108 (kPa)
I	6.452 x 10-4 (m^4)
W	73600 (N/m)
W_{DL}	19300 (N/m)
W_{LL}	54300 (N/m)

Special Limit State Functions

Series System

A series of 6 elements subjected to load Q is considered in this problem. The resistance of each element is considered to be independent. Since it is a series system, failure of the system occurs with failure of any one element in the series. For this problem, both resistance and load RV were considered as lognormally distributed with the resistance RVs having a mean of 10.0 and coefficient of variation (COV) of 0.10 and the load RV with a mean of 6.0 and COV of 0.10. Figure 4.2 shows a PDF estimate of the system resistance of the series system.
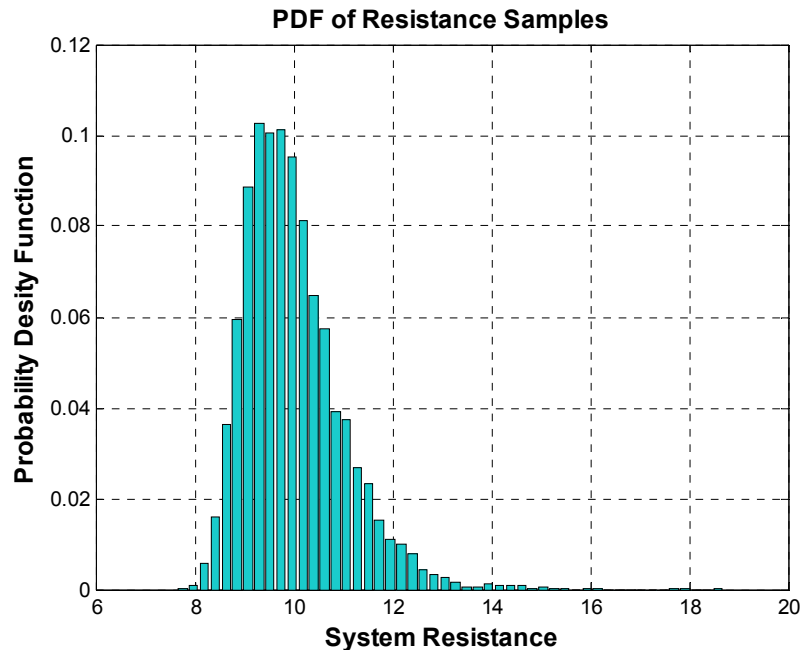
Figure 4.2 System Resistance of Series System

The limit state function is expressed as:

$$g = min(Ri) - Q \qquad (4.8)$$

The same limit state function was evaluated considering an extreme Type I distribution for resistance and load RVs. The mean load Q in this case was considered to be 1.5 with COV of 0.1.

Parallel System

For this problem, a system of 6 parallel elements was considered with resistance of each element independent and normally distributed with mean of 10 and COV of 0.10. The system is subjected to a load RV which was considered to be normally distributed with COV of 0.10. However, the mean load was varied from 40 to 70 in increments of 10 to produce various alternative functions.
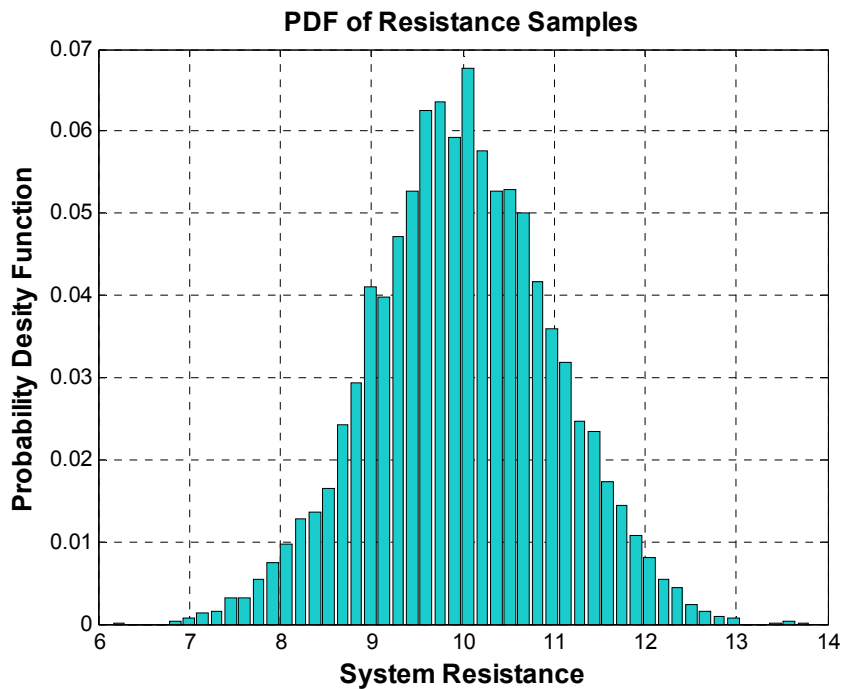
Figure 4.3 System Resistance of Parallel System

The limit state function is expressed as follows:

$$g = max(Ri) - Q/6 \tag{4.9}$$

The problem was reconsidered where all RVs were taken as lognormal and extreme I. However, for the lognormal case the mean load Q was taken as 45 and for the extreme I case the mean load was considered as 40.

Minimum Function

This is similar to the series system (1) and is expressed as the minimum of several sub-functions given by following expressions:

$$g = \min(g_1, g_2, g_3) \tag{4.10}$$

where:

$$g_1 = x_1 + 2x_2 + 2x_4 + x_5 - 5x_6 \tag{4.11}$$

$$g_2 = x_1 + 2x_2 + x_4 + x_5 - 5x_6 \tag{4.12}$$

$$g_3 = x_2 + 2x_3 + x_4 + x_5 - 5x_6 \tag{4.13}$$

RVs $x_1 - x_4$ are lognormal whereas x_5 and x_6 are extreme Type I. The means and standard deviations for RVs $x_1 - x_4$ are 60 and 6, respectively, while x_5 and x_6 have means of 20 and 25 and corresponding standard deviations of 6.0 and 7.5.

Maximum Function

This limit state function is similar to the parallel system (2) and is expressed as the maximum of several sub-functions given by the following expressions:

$$g = \max(g_1, g_2, g_{3,}g_4) \tag{4.14}$$

where:

$$g_1 = 2.677 - u_1 - u_2 \tag{4.15}$$

$$g_2 = 2.500 - u_2 - u_3 \tag{4.16}$$

$$g_3 = 2.323 - u_3 - u_4 \tag{4.17}$$

$$g_4 = 2.250 - u_4 - u_5 \tag{4.18}$$

All u_i are standard normal random variables.

Multiple Reliability Indices

This hyperbolic limit state function has two reliability indices, and is given as:

$$g = x_1 x_2 - 146.14 \tag{4.19}$$

where x_1 and x_2 are normal RVs having mean values of 78064.4 and 0.0104, with corresponding standard deviations of 11709.7 and 0.00156, respectively.

Circular Limit State

This is a two-dimensional limit state function (Figure 4.4) and is expressed by the equation given below. If solved using a reliability index-based method such as FORM, the problem has multiple (infinite) reliability indices as all points on the circle represent an equally shortest distance from the boundary of the limit state to the origin (assuming normal RVs). The limit state function is given as:

$$g = r^2 - \sum_{i=1}^{2} z_i^2 \tag{4.20}$$

Here z_i are standard normal and independent RVs whereas r represents the radius of the circular limit state function and is taken as a known quantity. For this problem, r is taken as 4 and z_1 or z_2 can be selected as the control variable as:

$$\widehat{z_1} = \sqrt{r^2 - z_2^2} \tag{4.21}$$

Here, MCS or MCMC are used to randomly assign values to z_2, where $\widehat{z_1}$ represents the system resistance sample and z_1 is the control variable. The reformulated limit state function can be expressed as:

$$\hat{g} = \widehat{z_1} - z_1 \tag{4.22}$$

The exact solution can be computed from the chi-square distribution as:

$$P_f = 1 - \chi_n(r^2) \tag{4.23}$$

where χ_n represents a chi-square distribution with n degrees of freedom.

Here, z_1 and z_2 are considered to be standard normal and independent whereas the radius r was varied from 4 to 8. For the FS method, z_1 was considered as a control random variable. The limit state function was reconsidered where all RVs were taken as lognormal and extreme I distributions. For the lognormal case the means and standard deviations of RVs were considered as 0.01 and 1.0 respectively, while for the extreme I case the means were considered to be 0 and the standard deviations 0.7. In both the lognormal and extreme type I case, the radius was considered as 6.0.
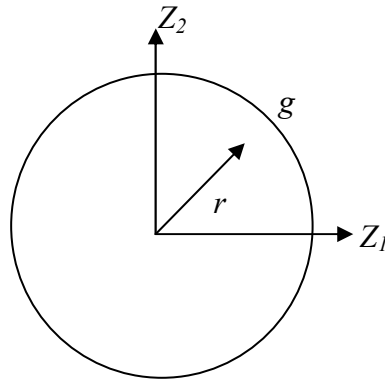
Figure 4.4 Shape of Circular Limit State Function

Analytical I-Beam

An analytical I-beam is subjected to a concentrated load as shown in Figure 4.5. This problem is taken from Acar et al. (2010). The limit state function is expressed in terms of bending stress as follows:

$$Y = \sigma_{max} - S \tag{4.24}$$

where:

$$\sigma_{max} = \frac{Pa(L-a)d}{2LI} \tag{4.25}$$

$$I = \frac{b_f d^3 - (b_f - t_w)(d - 2t_f)^3}{12} \tag{4.26}$$
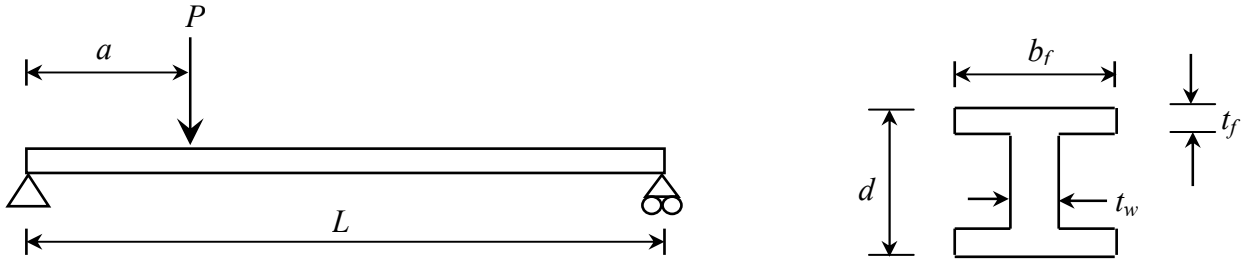
Figure 4.5. I-beam Cross-section and Loading

All RVs are normally distributed, with statistical parameters shown in Table 4.2. *S* was considered as the control variable, and the limit state function was reformulated as follows:

$$\hat{g} = \hat{S} - S \tag{4.27}$$

Table 4.2. Statistical Parameters for I-beam

RVs	Mean	Standard Deviation
P	6070 and 14000	200 and 460.6
L	120	6
a	72	6
S	17000	4760
d	2.3	1/24
b_f	2.3	1/24
t_w	0.16	1/48
t_f	0.16	1/48

Noisy Limit State Function

The following limit state was considered as a noisy limit state with a fluctuating failure boundary:

$$g = x_1 + 2x_2 + 2x_3 + x_4 - 5x_5 - 5x_6 + 0.001 \sum_{i=1}^{6} sin100xi \qquad (4.28)$$

All x_i were considered as lognormal. RVs x_1 through x_4 have means 120 and standard deviations of 12; RV x_5 has a mean of 50 with standard deviation of 15, and RV x_6 has a mean of 40 with standard deviation of 12.

Realistic Practical Engineering Problems

10 Bar Nonlinear Static Truss
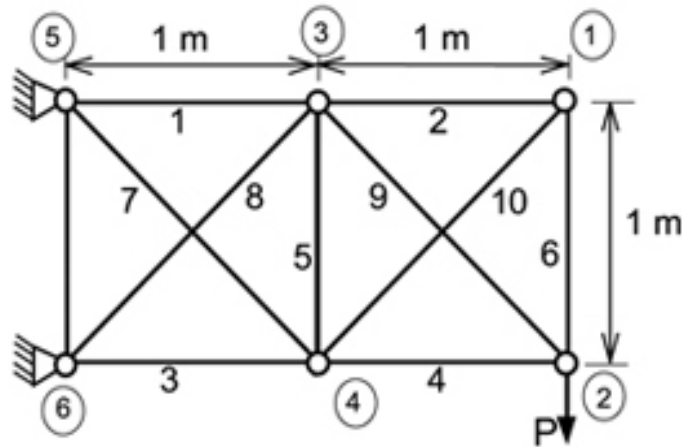
Figure 4.6 10 Bar Non-Linear State Truss

This problem is taken from Eamon et al; (2011) and Charumas (2008). Figure 4.6 shows a 10 bar, nonlinear static truss subjected to a load P. The complexity of the problem is such that a closed-form, analytical solution is unavailable. Thus, a commercial FEA code, ABAQUS (Version 6.11-2), was used to evaluate the limit state function. The limit state function for this particular problem was expressed in two different ways; in terms of displacement and in terms of stress. For the displacement limit state, only three RVs were considered for the problem by assuming similar material properties for all members. The material assumed was steel, with a bilinear stress-strain curve and an elastic modulus of elasticity E of 29,000 ksi. The yield stress (σ_y) was considered to be the same for all members, and hence is given as a single RV, with a mean of 50 ksi and COV of 0.10. The modulus of elasticity after yield i.e. post-yield

modulus (E_2) was given a mean of 1200 ksi and COV of 0.25. The load value P was varied from 45 to 55 kips, with a COV of 0.10. The failure condition was considered to be when the displacement under the point of application of load P exceeded 1.5 inches. Hence, the limit state function can be expressed as follows:

$$g = 1.5 - D(\sigma_y, E_2, P) \tag{4.29}$$

All RVs are taken as normally distributed. Load P was considered to be the control variable. The modified limit state function was then solved for the condition $g^* = 0$ using the bisection method. Although the limit state function was evaluated with a resistance sample size of 1000, the actual number of function calls exceeded 1000 because the iterative process of the root finding method makes multiple function calls to satisfy $g^* = 0$. The tolerance for error was taken as 0.01.

Further, to evaluate the FS method under more complex conditions, the limit state function was reformulated in terms of stress. In this case, the geometric and material properties were not considered the same for the entire structure. Rather, each member of the truss was given three independent RVs, thus increasing the number of RVs in the problem from 3 to 31. Additional RVs include the cross-sectional area A of each member, with a mean of 2 sq. in, and COV of 0.05. The mean and COV of yield stress σ_y and post yield modulus E_2 were kept the same as described in the displacement limit state function. However, these RVs were considered independent for each member in the structure. Mean load P was varied from 50 to 65 kips with COV of 0.1. It was again considered to be the control variable. The failure criteria was defined as the state when

the stress in member 1 reaches its yield value. The limit state function can be described as:

$$g = \sigma_{y1} - \sigma_1(P, \sigma_{yj}, E_{2i}, A_i) \text{ for } i = 1 \text{ to } 10, j = 2 \text{ to } 10 \qquad (4.30)$$

Steel Frame Structure
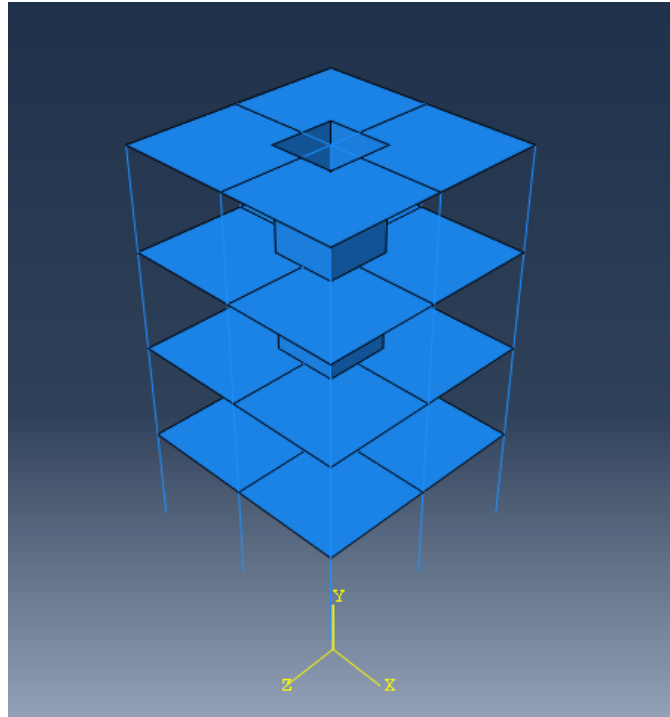
Figure 4.7 Steel Frame Structure

This problem considers a small structure representing a bay of a larger building, with dimensions 24 ft by 24 ft in plan and 48 ft high. It is a four-story steel frame, with concrete floor slabs and four interior shear walls, as shown in Figure 4.7. Note that it is idealized and not meant to model an actual structure. Beams and columns of the structure are modeled with line elements and assigned W14X22 steel section properties. The floor slabs and shear walls were modeled as shell elements, with slab thickness of 12 inches. A bilinear stress-strain model for steel was used, with RVs taken as modulus of elasticity of

steel, E_s, with mean of 29000 ksi and COV of 0.1; and post-yield modulus of elasticity of

steel, E_t, with mean of 1200 ksi and COV of 0.1. Additional RVs are modulus of

elasticity of concrete, E_c, with mean of 3500 ksi and COV of 0.1; and a uniform pressure

load applied to the floor slabs, which was taken as the control variable, with mean of 70

and 90 psi, depending on target reliability index considered, with COV of 0.1. The failure

criterion is defined as the state where displacement at any point on the fourth floor slab

exceeds 2 inches. The limit state function is given as:

$$g = 2 - D(E_s, E_t, E_c, P) \tag{4.31}$$

All RVs were taken as normally distributed. The limit state function was

evaluated using a commercial FEA code (ABAQUS).

Metal Automotive Structure

The model used for this validation problem was the Federal Highway

Administrations (FHWA) 'Bogie' model (available on the National Crash Analysis Center

(NCAC) website). This is a FEA model of a surrogate vehicle this is used for the full

scale crash test of highway appurtenances. The physical structure is used to simulate the

impact dynamics of a small vehicle and can be configured with different noses to

represent alternate crash scenarios (Eskandarian et al. 1997). A schematic sketch of the

test vehicle is shown in Figures 4.8 and 4.9, while the material properties used in the

model are shown in Table 4.3.

The crash scenario analyzed with the Bogie model is a small car impacting a rigid pole. Here, the simulated nose structure is considered for low speed impacts (32 km/hr). Figures 4.8 and 4.9 show the model before a representative impact.
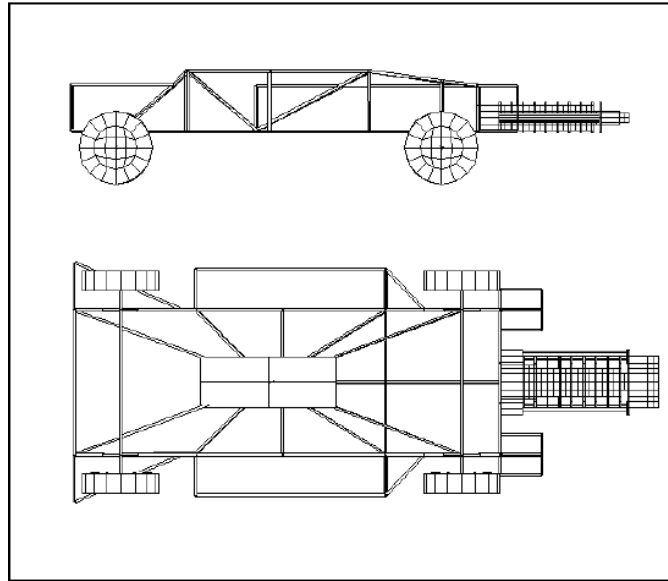
Figure 4.8 Schematic of FHWA Bogie Model (Eskandarian et al 1997)

Table 4.3. Material Properties (RVs) for Bogie (Eskandarian et al 1997)

Type & Number of Elements	Parts	Young's Modulus (MPa)	Poisson's Ratio	Density (kg/mm^3)	Yeild Stress (MPa)
Beam (126)	Structural Beams	20×10^4	0.3	0.785×10^{-5}	207
Shell (384)	Steel Plates	20×10^4	0.3	0.785×10^{-5}	207
	Steel Hub	20×10^4	0.3	0.785×10^{-5}	207
	Rubber Tire	2.46×10^3	0.323	0.106×10^{-5}	24.77
Solid (1286)	Instruments Box	1.25×10^4	0.33	0.785×10^{-5}	207
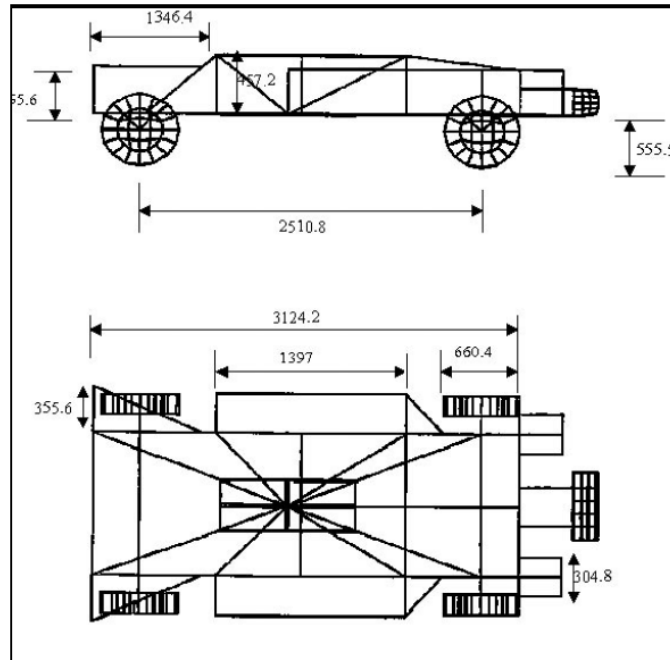
Figure 4.9 Schematic of FHWA Bogie Model (Eskandarian et al 1997)

Marine Structure

A submarine sail structure with length, width and height of 100 ft x 20 ft x 20 ft, respectively, is considered for analysis (Figure 4.10). This structure is composed of a thick outer composite shell reinforced with stiffeners, and taken from Eamon et al. (2008). The structure is divided in to four main components; the crown, transition region, main skin, and the base joint. The crown is made of a thick layer of steel, whereas the transition and main skin regions are made of bi-directional glass reinforced polymer (GRP). The sail is subjected to a critical waveslab load. To support the waveslab load, the composite skin is stiffened by four longitudinal and eight transverse stiffeners. The FEA model was originally modeled in MD Nastran by Eamon et al (2008). For the purpose of this research, however, the model was remeshed and solved in ABAQUS 6.11. The original model was composed of steel and GRP composite with linear elastic properties.

However, as a linear-elastic material, it was gauged insufficiently nonlinear with regard to response, and thus for this study, the entire sail structure was remodeled with steel assuming a bilinear stress strain curve, with mean elastic modulus E of 29,000 ksi with a COV of 0.1. The yield stress (σ_y) was considered the same for the crown, main skin, and the stiffeners and hence was assumed to be a single RV with mean of 50 ksi and COV 0.1. Similarly, the post-yield modulus (E_2) was considered to have a mean of 1200 ksi and COV of 0.25. The transient waveslab caused by an ocean wave striking the sail on one side was modeled as an equivalent static uniform load on the side of the sail.
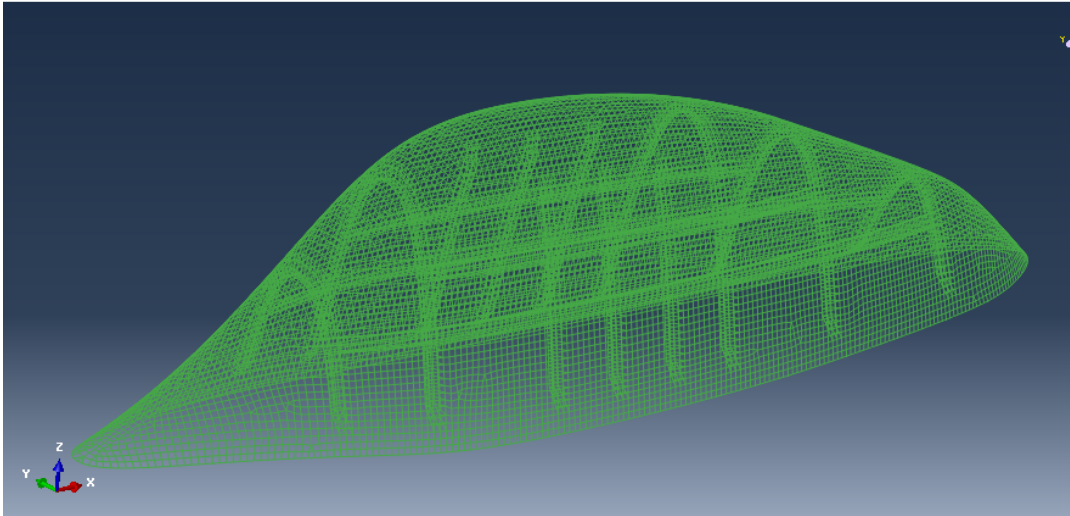
Figure 4.10 Mesh of Marine Sail Structure

Masonry Building Structure

This problem represents the response of an exterior masonry infill wall exposed to blast. This problem is highly non-linear with large strain and large displacements that include arbitrary element contact and material disintegration under very high strain rates. Although originally solved by Eamon et al. (2007) in DYNA3D, for this study, the model was remeshed and solved using ABAQUS 6.11. Here, the CMU walls were considered

to be fully filled with grout. The walls are composed of 15 rows of standard 8x8x16 nominal CMUs producing a wall height/thickness aspect ratio of 15:1. The wall behaves similarly to a plane-strain condition and hence is modeled using unit length stack of CMU blocks. The topmost and the bottommost blocks are modeled as fixed ends representing a condition of a floor above and beneath. Previous work on this problem demonstrated that CMU interconnectivity and contact parameters along joint lines govern over individual block deformations. Therefore, except for the end CMU blocks which rest against the supports, the interior blocks were modeled using a single element each. However, the end blocks were modeled using a finer mesh, which was required to accurately model the progressive material crushing that occurs where the wall contacts the floor and ceiling, caused by the outward rotation of the wall. The coefficient of friction between the CMU surfaces was taken as 0.50. Material properties were taken from Eamon et al. (2007). Blast load was applied as a dynamic load as a time varying, uniform pressure over the entire wall as shown in Figure 4.11. The load curve is idealized by four piece-wise linear functions, two positive and two negative. Four RVs are used to describe the load curve and the respective values are shown in Table 4.4. The RV variation originates from three primary sources; expected standoff distance, charge weight, and the variation in the explosive material itself. For the purpose of reliability analysis, pressure is expressed as a load RV while mortar joint strength, block-block joint friction, upper block-frame friction and lower block-frame friction are considered as resistance RVs, and are given in Table 4.5. However, the mortar joint strength and block-block joint friction are considered RVs for only the (generally) three most-critical center

CMU blocks. The limit state is written in terms of a critical debris velocity which may cause serious injuries to building occupants. The critical debris velocity, V for this problem was taken as 11.5 m/s (37.72 ft/s). Figure 4.12 shows the FEA model undeformed CMU wall.

Figure 4.11 Load Curve Random Variables	Figure 4.12 FEA Model of Section of CMU
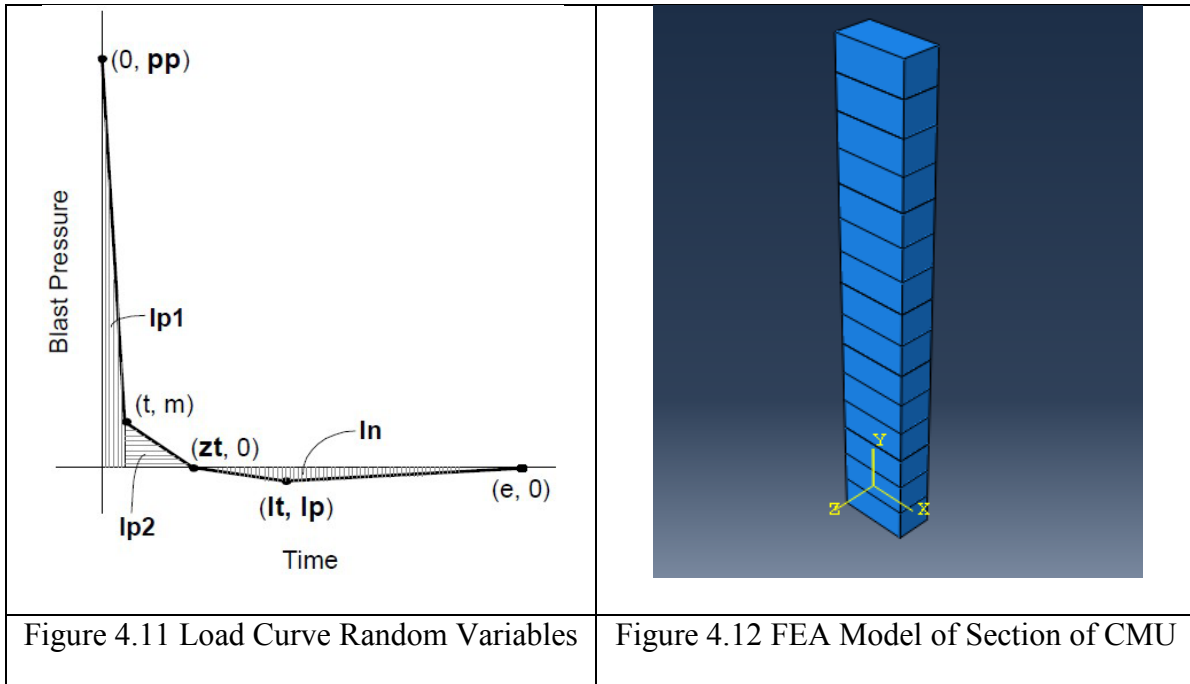
Table 4.4. Load & Resistance RVs

Random Variable (RV)	Mean	COV
Zero Pressure Time (zt)	2.16	0.13
Peak Pressure (pp)	1518	0.24
Low Pressure (lp)	-25.3	0.18
Low Pressure time (lt)	3.73	0.13
Mortar Joint Strength	1.73	0.24
Block-block joint friction	0.5	0.11
Upper block-frame friction	0.65	0.11
Lower block-frame friction	0.65	0.11

CHAPTER 5 RESULTS AND DISCUSSION

This chapter presents the results obtained from the various FS implementations explored and some other reliability analysis techniques by solving the analytical and realistic engineering problems discussed in Chapter 4. However, in order to facilitate a comparison between numerical integration and the different curve fit techniques, it is necessary to explore the effect on number of intervals on the accuracy of NI itself. Hence, the first section of this chapter discusses the effect of interval size on the accuracy of the NI method and thereby on FS. The second section presents the results obtained from the analytical functions whereas the third section discusses the realistic engineering problems and the results obtained from the same. The fourth and last section discusses the results obtained by implementing MCMC method to generate $R(X_i)$ sample instead of crude MCS.

Effect of Interval Size on Accuracy of FS Method

As explained in Chapter 3, the simplest way to calculate p_f is expressed as follows:

$$p_f = \int_{-\infty}^{\infty} F_R(x) f_q(x) dx \tag{5.1}$$

$$p_f = \sum_{i=1}^{N} F_R(q_i) \times f_q(q_i) \times dq \tag{5.2}$$

The above expression is evaluated using numerical integration (NI). This evaluation requires that the PDF of the resistance samples is determined; an evaluation that is conducted with the interval method. Here, the resistance samples are divided into

specific intervals and then the number of data points that fall into each interval is counted, and the results normalized to produce the PDF. However, the accuracy of the PDF estimate depends on the number of intervals. As the number of intervals are changed, the resulting PDF changes, which in turn affects the calculated probability of failure.

Hence, the various limit state functions (general and special limit state functions) described in Chapter 4 were evaluated considering different interval sizes in order to determine the optimum number of intervals for developing the PDF of resistance. The PDF of resistance was constructed by varying the number of intervals from 5, 10, 50, 100, and 500. In each case, the number of resistance samples $R(x_i)$ was kept at 1000. Probability of failure was then calculated using eq. (5.2) for each case and compared with the exact solution obtained from direct Monte Carlo Simulation (MCS). Figures 5.1 and 5.2 show the results for selected limit state functions. It was observed that 50 intervals for 1000 resistance samples $R(x_i)$ provided consistently good results for most limit state functions. Also, it was found for relatively linear limit state functions and for those with few random variables, an insignificant difference in percentage error was observed when interval size was changed from 50 to 500. However, with an increase in the number of random variables and for highly non-linear limit state functions, the error in probability of failure significantly increased as interval size deviated from 50. Figures 5.3 and 5.4 show the error from constructing the PDF using 10 and 50 intervals for a 5 RV non-linear problem, while Figures 5.5 and 5.6 show the difference from using 10 and 50 intervals for constructing the PDF. These figures clearly indicate that a change in interval size can

significantly affect the probability of failure estimation. It was also observed that a small change in the interval size did not produce large differences in the results. For example; changing interval size from 50 to 60 had an insignificant impact on the precision of results.

Results of the interval method for all limit state functions considered are presented in the next section. In this section, for all limit state function evaluations using the NI method, 1000 resistance samples and 50 intervals were considered for PDF construction. The NI method produced good results for most of the high and low reliability index cases. In a few cases, it was observed that the NI method produced high reliability indices for RVs with a lognormal distribution. It was also observed in some cases that NI failed to produce results where the RVs had 5% COV with either normal or lognormal distributions, usually for the cases with high reliability index. Moreover, error generally increases or the method fails to produce results where the function has high target reliability index and is highly non-linear with 15 RVs.
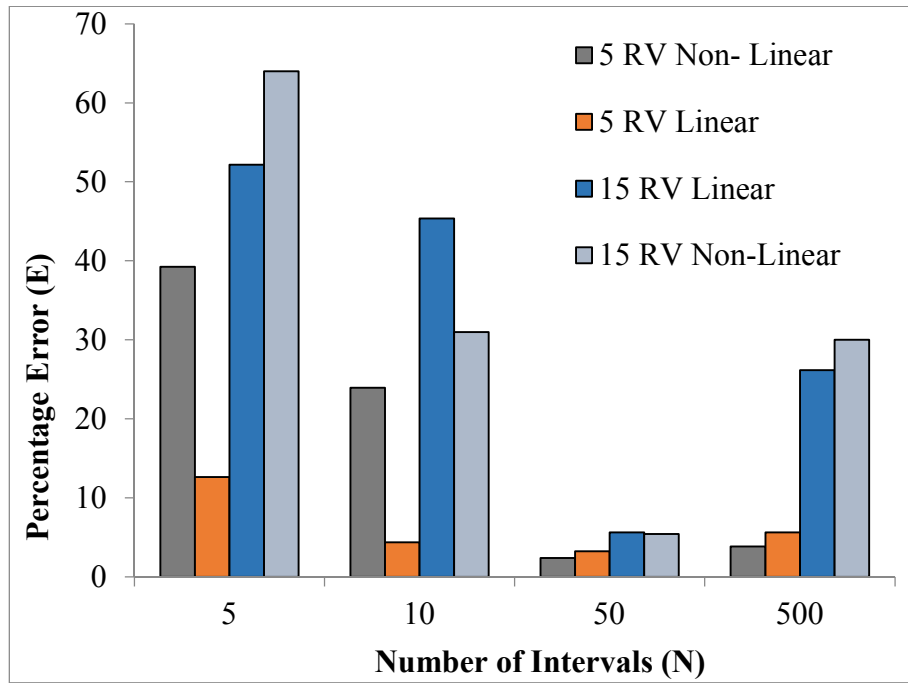
Figure 5.1 Number of Intervals vs Error for General Limit State Functions
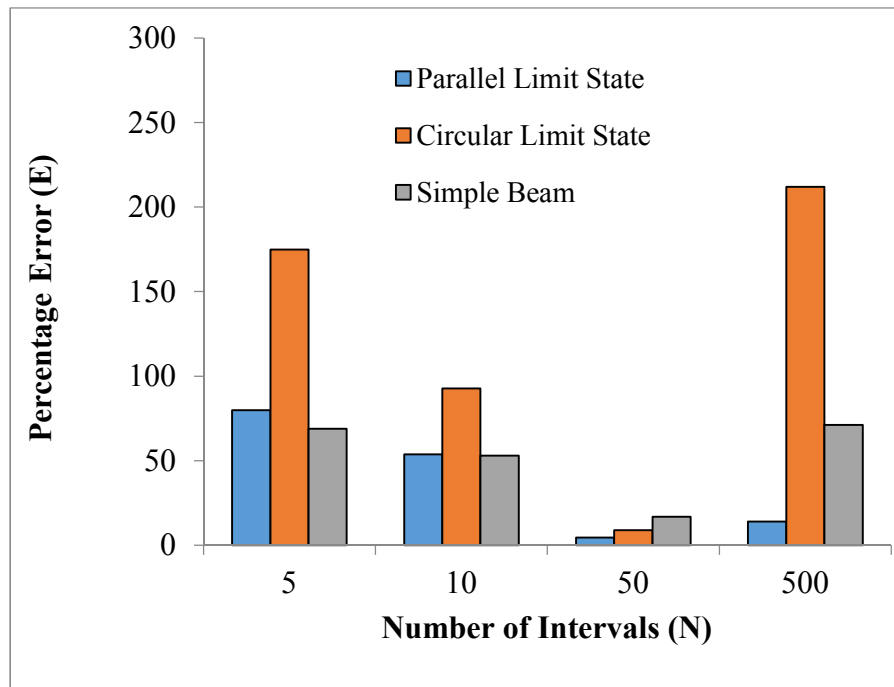
Figure 5.2 Number of Intervals vs Error for Special Limit State Functions
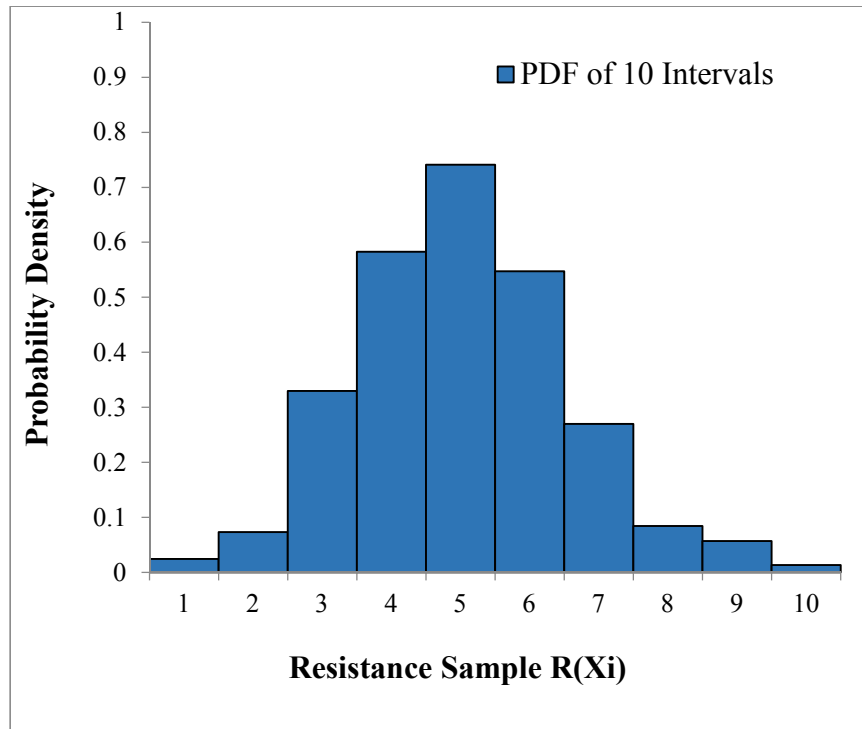
Figure 5.3. PDF of 10 Intervals for a 5 RV Non-Linear Problem
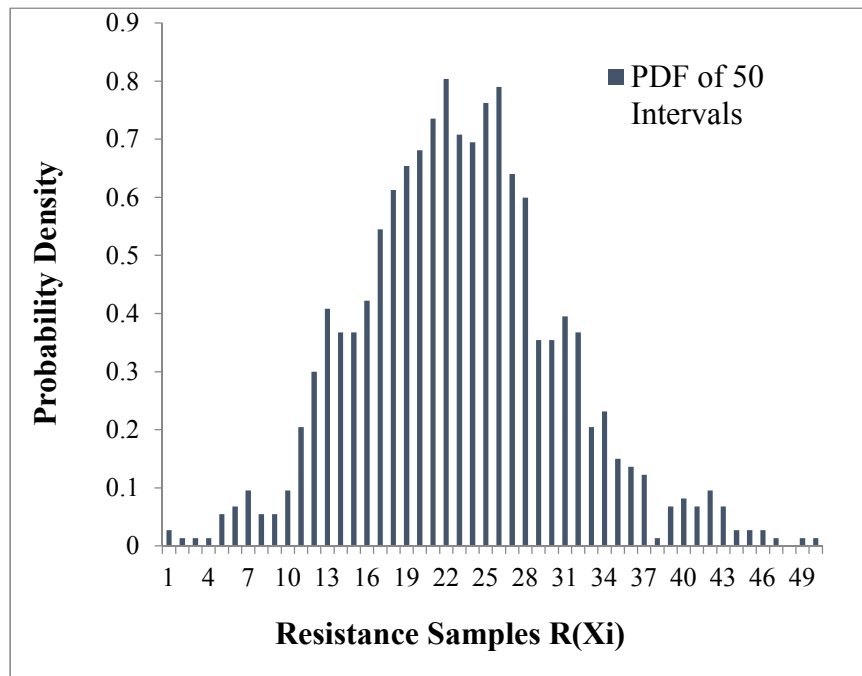
Figure 5.4. PDF of 50 Intervals for a 5 RV Non-Linear Problem
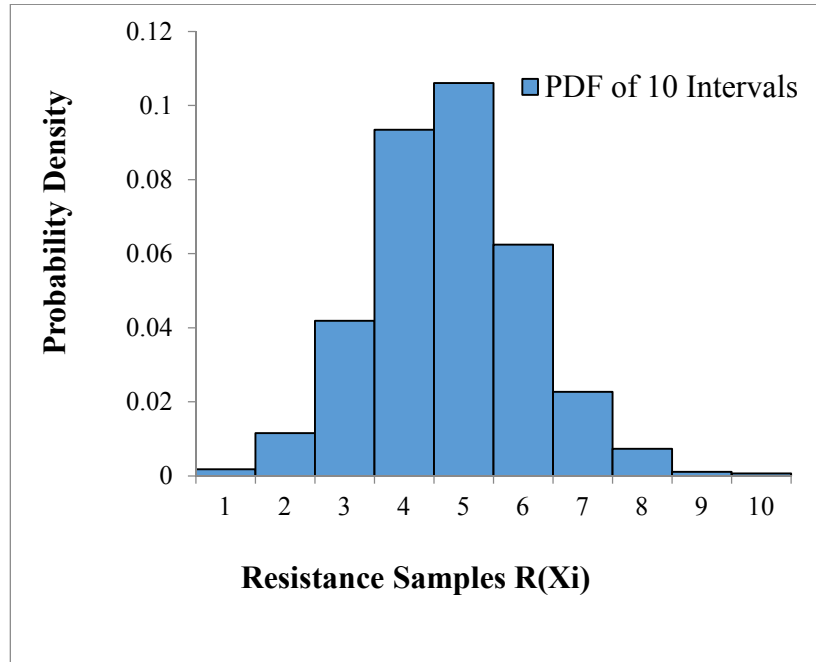
Figure 5.5. PDF of 10 Intervals for Parallel System
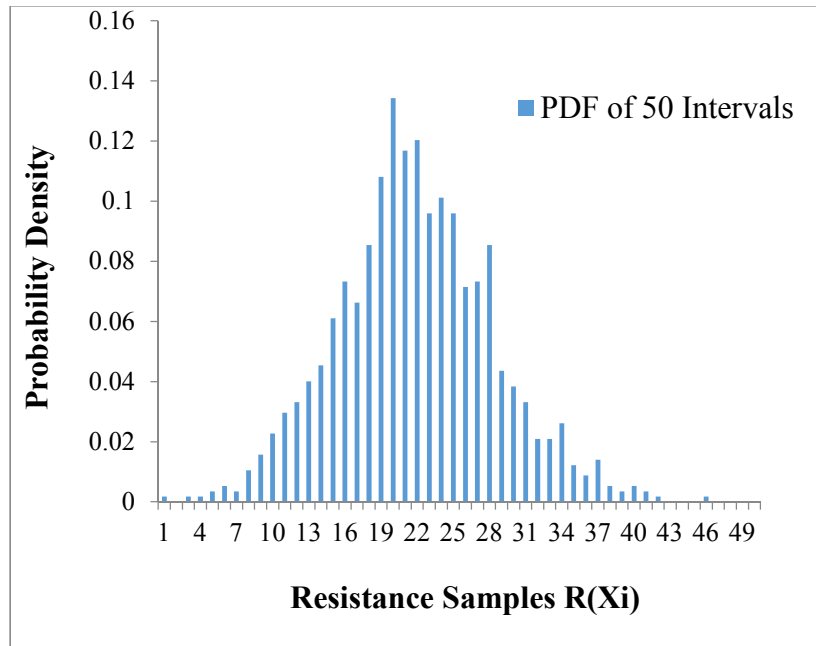
Figure 5.6. PDF of 50 Intervals for Parallel System

General Limit State Function

As explained in Chapter 4, the general limit state function comprised of 96 different variations which consider the effect of number of RVs, COV, type of distribution and target reliability index on the accuracy of the FS implementation approaches. All cases were evaluated using the NI, GLD, JSD, GEV and ensemble methods. Results are measured in terms of accuracy and precision, where accuracy is the mean value of the ratio of computed reliability index to the exact value for the specific case under consideration. Here the exact value for low to moderate target reliability indices is determined from 1×10^6 MCS simulations. However, for high target reliability index cases the exact value is determined from 1×10^9 MCS simulations. Precision is used to measure the degree of consistency of results, and is determined by calculating the COV of accuracy, based on five evaluations of each problem. Figures 5.7 - 5.12 show the effect of number of RVs, degree of non-linearity, and RV distribution type on the different implementation methods.

Effect of FS Implementation Methods On Accuracy and Precision

Table 5.1 presents the results obtained from various FS implementation methods described in Chapter 3. It can be observed that the GLD method provides good results for low reliability indices. For high reliability levels, however, the GLD tends to either fail or produce unstable results. Also, it can be observed that the GLD provided good results for almost all of the extreme Type I distribution limit states.   It was also observed in some cases that the GLD failed to produce results where the RVs had 5% COV with either normal or lognormal distributions. These are usually the cases with high reliability

index. Moreover, error generally increases or the method fails to produce results where the function has high target reliability index and is highly non-linear with 15 RVs. For the functions with low target reliability indices, the GLD produced good results irrespective of the non-linearity and number of RVs.

The EGLD method was unable to provide good fits for limit states with a high reliability index. One of the reasons that the EGLD method provides poor or no results in some cases is due to the (α^2_3, α_4) space covered by the EGLD. It was observed that computations become numerically difficult when the (α^2_3, α_4) values within the EGLD region gets close to the boundaries. It was also observed that as α_4 approaches the value of $\alpha_4 = 3 + 2 \alpha^2_3$, which is the upper boundary of the EGLD region, determination of EGLD parameters becomes difficult numerically. However, as α_4 approaches the upper boundary, it also gets closer to the GLD region and hence the GLD provides good results in these cases and EGLD is most likely to fail. The results shown in Table 5.2 are for cases where the EGLD was able to fit to the resistance samples for the general limit state function. Figures 5.7 and 5.8 show the comparison of the EGLD fit with that of the raw PDF obtained from the resistance sample.

Table 5.1. Reliability Indices for General Limit State Function using NI, GLD, JSD,

GEV& Ensemble Approach

Limit State	RV distribution	COV	Target β	Beta					
				NI	GLD	JSD	GEV	Ensemble	MCS
2 RV Linear	Normal			4.520	Fail	4.264	Fail	4.463	4.360
	Lognormal	0.05	Low	3.380	Fail	4.265	Fail	4.265	4.420
	Extreme			1.002	0.859	0.872	0.874	0.989	1.009
2 RV Linear	Normal			1.422	0.625	0.626	0.614	0.634	0.620
	Lognormal	0.35	Low	2.410	0.640	0.662	0.644	0.665	0.650
	Extreme			1.002	Fail	0.974	0.995	0.989	0.990
2 RV Non-Linear	Normal	0.05	Low	2.293	2.315	2.284	2.196	2.164	2.279
	Lognormal			Fail	2.144	2.273	2.159	2.236	2.190
	Extreme			1.089	0.917	0.919	0.913	0.894	1.024
2 RV Non-Linear	Normal	0.35	Low	0.686	0.285	0.284	0.276	0.284	0.283
	Lognormal			2.078	0.434	0.431	0.445	0.428	0.440
	Extreme			0.973	0.812	0.840	0.816	0.875	0.987
5 RV Linear	Normal			3.105	2.929	2.947	3.079	2.959	2.953
	Lognormal	0.05	Low	1.212	NF*	4.108	Fail	4.108	4.021
	Extreme			3.699	NF*	3.719	Fail	3.695	3.763
5 RV Linear	Normal			0.884	0.884	0.920	0.882	0.967	0.941
	Lognormal	0.35	Low	3.300	0.880	0.997	0.985	0.987	0.977
	Extreme			0.960	0.839	0.934	0.905	0.964	0.951
5 RV Non-Linear	Normal	0.05	Low	1.770	2.090	2.079	2.142	2.064	2.072
	Lognormal			0.616	2.040	2.035	2.084	2.002	2.023
	Extreme			1.042	0.843	0.923	0.836	0.923	1.056

Table 5.1.a Reliability Indices for General Limit State Function using NI, GLD, JSD,

GEV& Ensemble Approach (Continued)

Limit State	RV distribution	COV	Target β	Beta					
				NI	GLD	JSD	GEV	Ensemble	MCS
5 RV Non-Linear	Normal	0.35	Low	Fail	Fail	0.349	0.382	0.385	0.397
	Lognormal			1.718	0.379	0.369	0.376	0.366	0.372
	Extreme			0.905	Fail	0.986	1.036	1.050	0.991
15 RV Linear	Normal	0.05	Low	3.505	NF*	3.432	Fail	3.484	3.751
	Lognormal			1.056	NF*	3.599	Fail	3.616	3.838
	Extreme			0.898	0.912	0.884	0.782	0.886	0.892
15 RV Linear	Normal	0.35	Low	2.351	1.049	1.075	0.982	0.982	0.968
	Lognormal			0.636	1.017	0.988	1.003	0.985	0.980
	Extreme			0.914	0.955	0.938	0.824	0.967	0.929
15 RV Non-Linear	Normal	0.05	Low	2.117	Fail	3.089	3.325	3.115	3.162
	Lognormal			0.710	Fail	2.727	3.105	2.999	3.058
	Extreme			0.785	0.790	0.759	0.755	0.792	0.811
15 RV Non-Linear	Normal	0.35	Low	Fail	Fail	1.762	0.415	1.757	1.801
	Lognormal			Fail	Fail	1.717	0.903	1.686	1.7896
	Extreme			0.414	Fail	0.364	0.187	0.382	0.361

Table 5.1.b Reliability Indices for General Limit State Function using NI, GLD, JSD,

GEV& Ensemble Approach (Continued)

Limit State	RV distribution	COV	Target β	Beta					
				NI	GLD	JSD	GEV	Ensemble	MCS
2 RV Linear	Normal			3.135	Fail	3.349	Fail	3.453	3.695
	Lognormal	0.05	High	Fail	3.540	4.105	Fail	4.405	4.052
	Extreme			3.016	2.863	2.878	2.799	2.916	3.030
2 RV Linear	Normal			1.370	1.381	1.317	1.360	1.378	1.377
	Lognormal	0.35	High	1.610	Fail	1.530	1.543	1.534	1.576
	Extreme			3.005	2.972	2.929	2.565	2.982	2.965
2 RV Non-Linear	Normal	0.05	High	3.532	Fail	3.719	Fail	3.664	3.791
	Lognormal			1.155	0.816	0.816	0.820	0.800	0.799
	Extreme			3.140	2.968	3.036	2.911	2.949	3.032
2 RV Non-Linear	Normal	0.35	High	1.160	Fail	0.664	0.653	0.656	0.675
	Lognormal			2.147	0.807	0.801	0.809	0.803	0.799
	Extreme			2.968	2.911	2.948	2.770	2.862	2.994
5 RV Linear	Normal			2.666	3.432	3.195	3.432	3.441	3.375
	Lognormal	0.05	High	1.380	Fail	3.927	Fail	3.927	4.222
	Extreme			6.461	2.929	2.628	3.012	2.898	2.872
5 RV Linear	Normal			0.287	1.697	1.731	1.804	1.731	1.745
	Lognormal	0.35	High	1.932	1.908	1.955	2.042	1.936	1.964
	Extreme			2.900	2.044	2.018	2.049	1.899	1.972
5 RV Non-Linear	Normal	0.05	High	3.333	Fail	3.121	3.432	3.262	3.274
	Lognormal			0.743	3.719	3.846	3.629	3.778	3.916
	Extreme			2.819	2.968	3.062	2.894	2.986	3.067

Table 5.1.c Reliability Indices for General Limit State Function using NI, GLD, JSD,

GEV& Ensemble Approach (Continued)

Limit State	RV distribution	COV	Target β	Beta					
				NI	GLD	JSD	GEV	Ensemble	MCS
5 RV Non-Linear	Normal	0.35	High	Fail	Fail	0.866	0.835	0.855	0.819
	Lognormal			*	*	1.009	0.981	0.949	0.939
	Extreme			Fail	2.911	3.090	2.948	2.948	3.003
15 RV Linear	Normal	0.05	High	2.050	3.346	NF*	3.540	3.540	3.534
	Lognormal			0.816	3.186	3.090	3.290	3.182	3.162
	Extreme			0.884	NF*	1.006	0.939	0.950	0.892
15 RV Linear	Normal	0.35	High	0.940	2.335	2.416	2.524	2.352	2.501
	Lognormal			1.933	2.896	2.527	2.848	2.882	2.802
	Extreme			0.934	0.910	0.898	0.934	0.901	0.929
15 RV Non-Linear	Normal	0.05	High	Fail	Fail	1.776	1.798	1.792	1.766
	Lognormal			Fail	Fail	1.871	1.739	1.743	1.739
	Extreme			Fail	NF*	2.590	2.457	2.601	2.639
15 RV Non-Linear	Normal	0.35	High	Fail	Fail	0.276	0.161	0.270	0.266
	Lognormal			Fail	Fail	0.401	0.212	0.386	0.390
	Extreme			Fail	Fail	1.943	1.103	1.943	1.976

Table 5.2. EGLD Results for Selected General Limit State Functions

Limit State	RV distribution	COV	Reliability Index (Beta)		
			GLD	EGLD	MCS
2 RV Linear	Normal		0.625	0.545	0.620
	Lognormal	0.35	0.640	Fail	0.650
	Extreme		Fail	1.710	0.990
2 RV Non-Linear	Normal		2.315	1.480	2.279
	Lognormal	0.05	2.144	1.603	2.190
	Extreme		0.917	Fail	1.024
5 RV Linear	Normal		0.884	0.423	0.941
	Lognormal	0.35	0.880	Fail	0.977
	Extreme		0.839	Fail	0.951
5 RV Non-Linear	Normal		Fail	3.092	3.274
	Lognormal	0.05	3.719	3.068	3.916
	Extreme		2.968	Fail	3.067
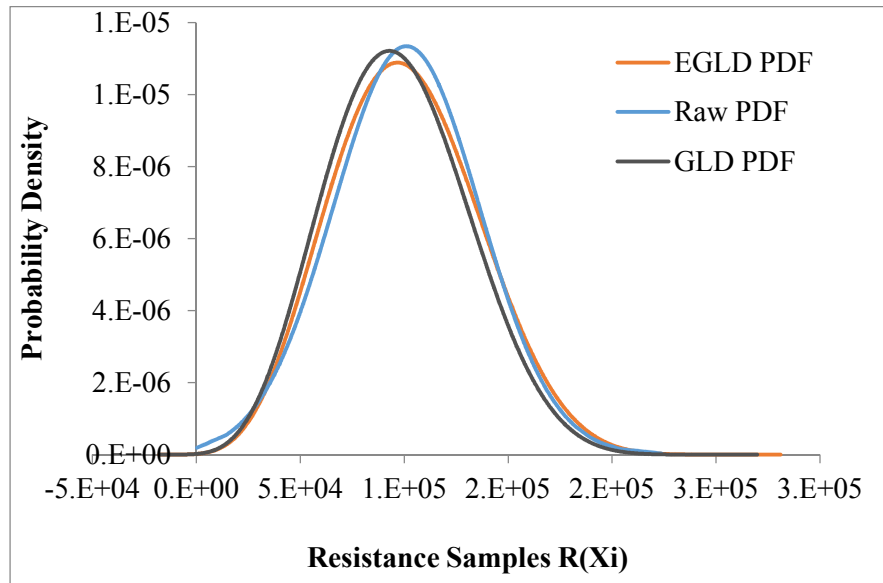
Figure 5.7 Comparison of EGLD PDF and Raw PDF of a 2 RV Normal Function
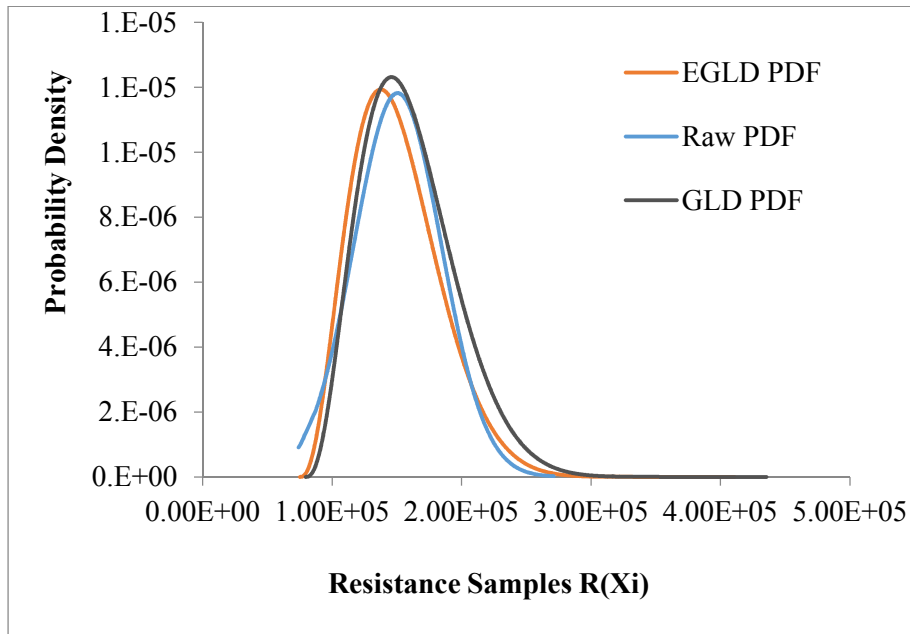
Figure 5.8 Comparison of EGLD PDF and Raw PDF of a 5 RV Lognormal Function

From the results presented in Table 5.1 it can be observed that the FS method coupled with JSD produced the most accurate and precise results. Surprisingly, the cases where JSD yielded the least accuracy and precision were linear limit state functions. However, these limit states were those corresponding to 15 RVs and high beta values. On the other hand, although GEV did not generally produce highly accurate results, it did produce consistent results. It was also found that GEV failed to produce any results for high beta values. Further, for most of the low beta value cases having normal and lognormal distributions, GEV produced poor results. This can be seen in Figures 5.13 and 5.14 where GEV resulted in low accuracy and high precision for low beta and normal distribution cases. It was observed that for almost all the cases with lognormal RVs, NI produced poor results, although it produced good results for almost all of the special limit states considered. Further, the precision of NI was degraded with nonlinear problems.

However, no specific pattern in the results was observed for GLD, although it produced

poor or no results for the 15 RV non-linear limit states.
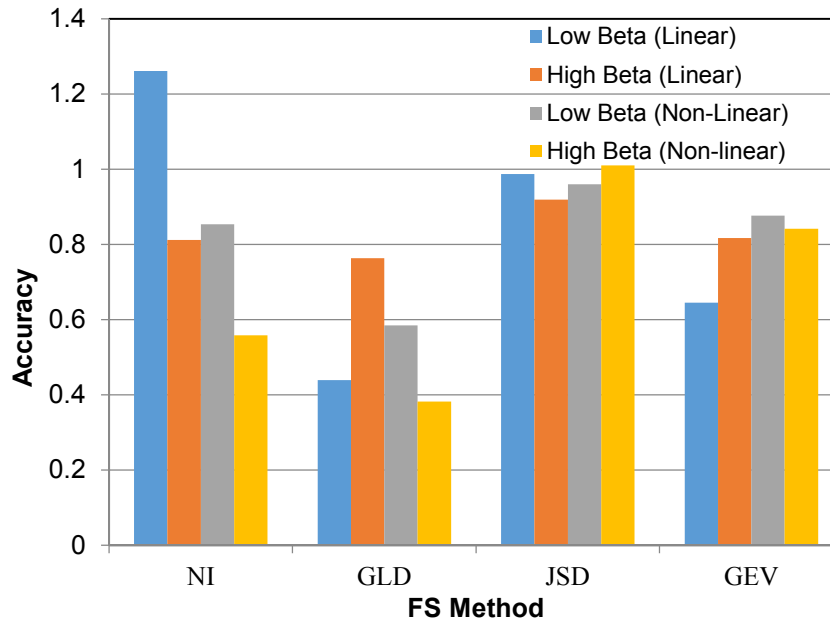
Figure 5.9 Effect of Linearity on Accuracy of FS Method
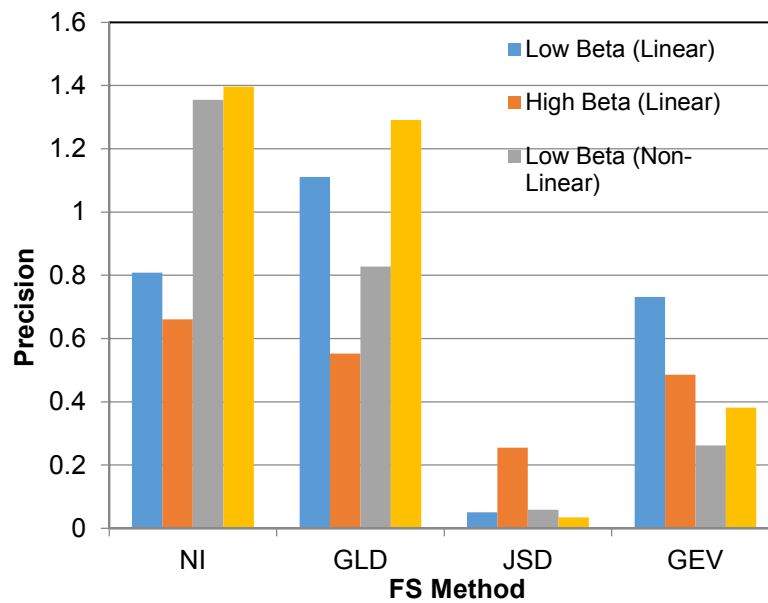
Figure 5.10 Effect of Linearity on Precision of FS Method
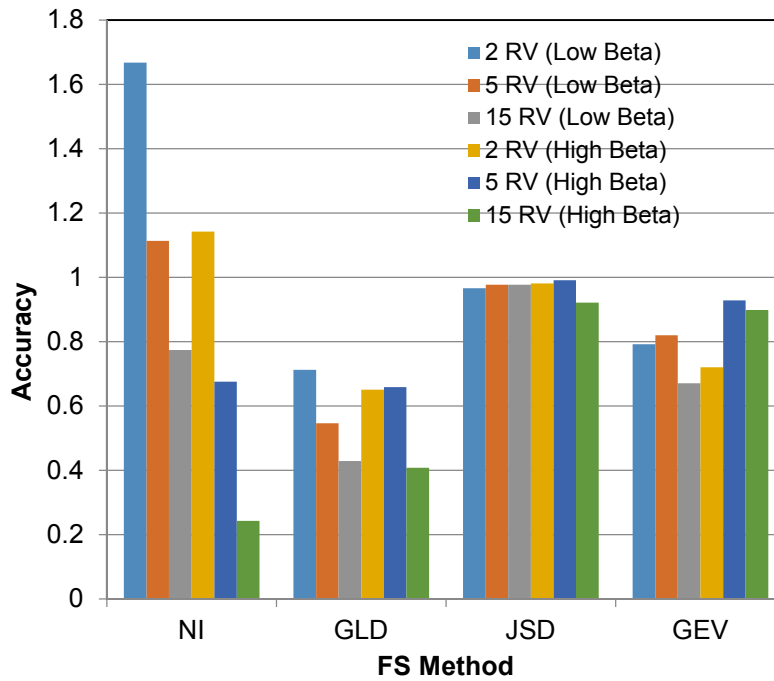
Figure 5.11 Effect of Number of RVs on Accuracy of FS Method
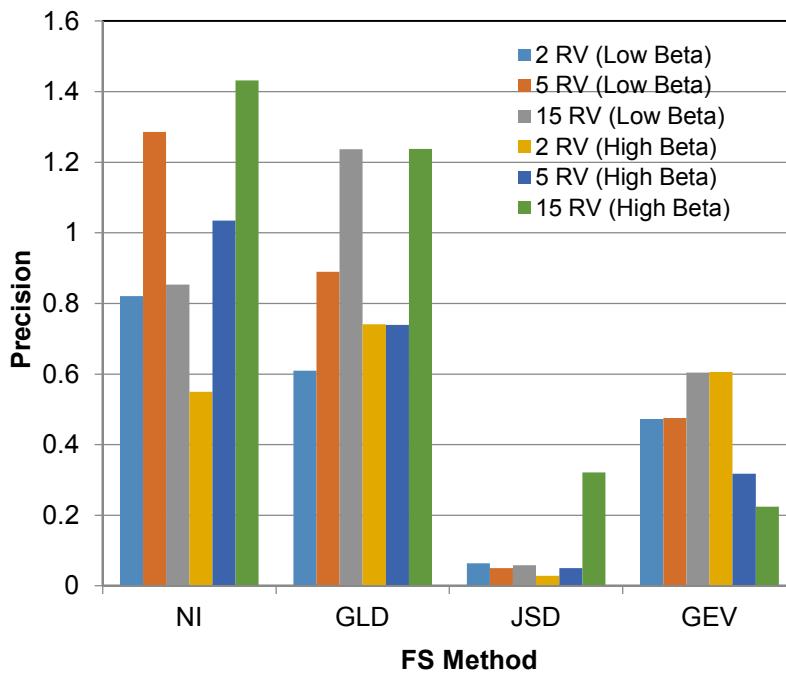
Figure 5.12 Effect of Number of RVs on Precision of FS Method
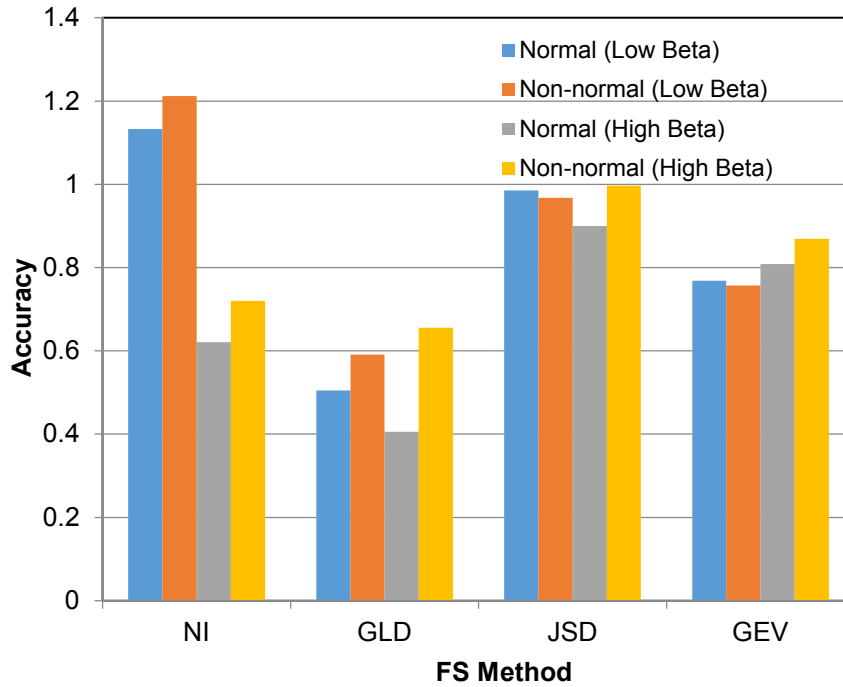
Figure 5.13 Effect of Normality on Accuracy of FS Method
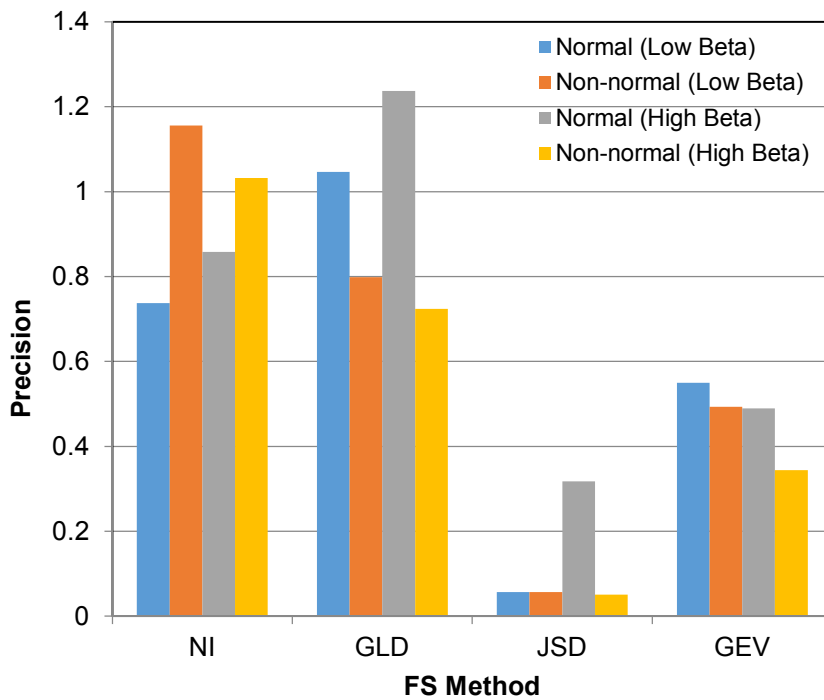
Figure 5.14 Effect of Normality on Precision of FS Method

Effect of Ensemble Implementation Method On Accuracy and Precision of FS

All the limit states described Chapter 4 were evaluated using the optimized ensemble technique. Results are presented in Table 5.1. It was observed that the application of the ensemble technique reduced the percent error in some cases, while in other few cases there was an insignificant difference observed between the stand-alone methods and the ensemble results. There were a few cases where the ensemble technique produced poor results. However, these were the cases where the error estimate from all the stand-alone methods was high and the ensemble could not produce significant improvement. For cases where only one stand-alone method produced acceptable results and the remaining methods either failed or produced high error estimates, it was observed that ensemble produced the same results as the most-accurate stand-alone method. This is because, during the optimization process, the highest weight factor is alloted to the stand-alone method which produced a CDF closest to the true CDF. However, no specific pattern was observed for the cases where the ensemble method failed to show significant improvement as compared to stand-alone methods. Figures 5.15 and 5.16 show a comparison between the CDF obtained from the ensemble method and other stand-alone methods.
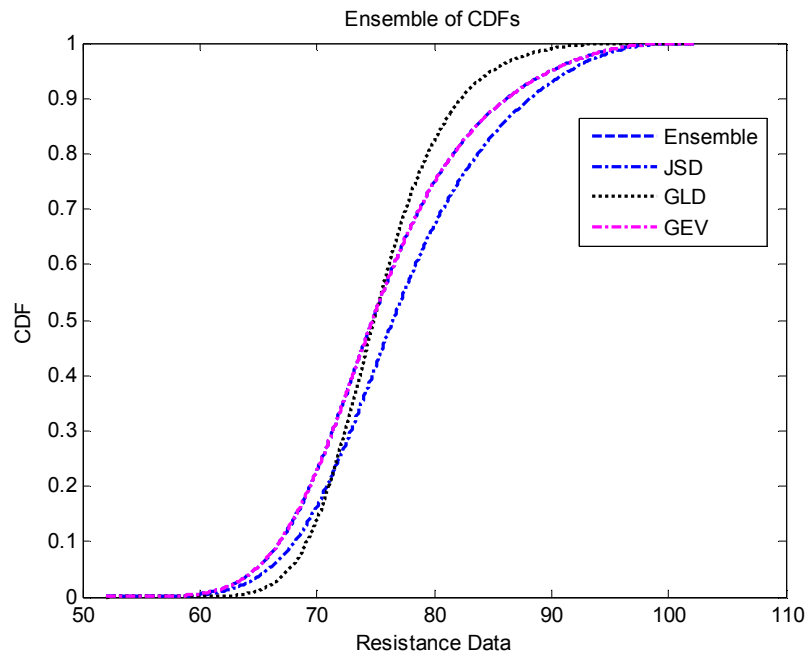
Figure 5.15 Ensemble of CDFs for a 5 RV Linear Limit State
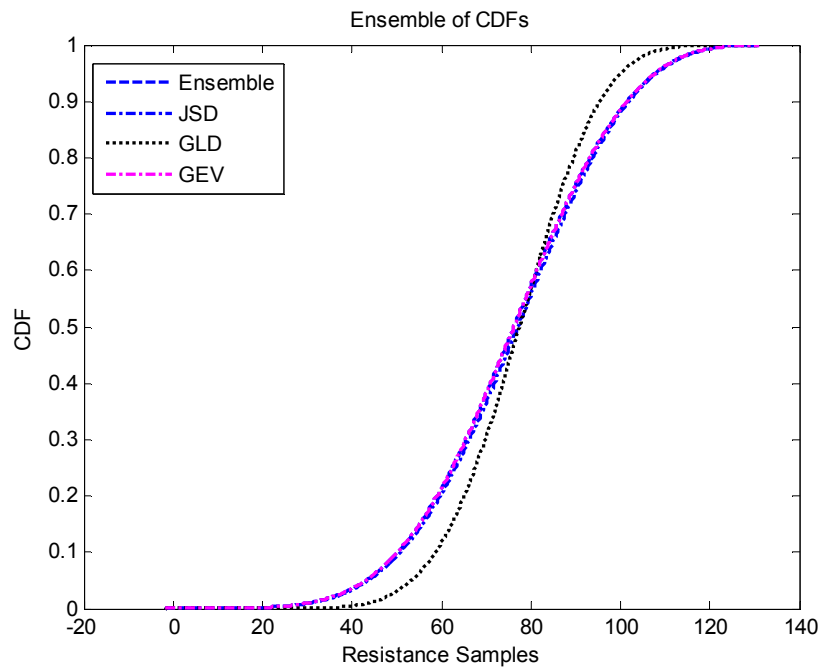
Figure 5.16 Ensemble of CDFs for a 5 RV Non-Linear Limit State

Special Limit State Functions

Series System

For this case, 'Q' was considered as the control variable for the FS method. The exact solution was obtained using 1×10^6 MCS samples. The results shown in Table 5.3 indicate that NI failed to provide results for both lognormal and extreme I cases. JSD and GEV produced good results for the lognormal case but produced higher errors for the extreme I case. However, GLD provided good results for both cases. MCS with 1000 calls to the limit state produced no failures.

Table 5.3. Series System

	all RVs are:	Lognormal		Extreme I	
Method	no. of calls	β	%err	β	%err
Exact solution		3.13	--	3.05	--
MCS	1000	N.F.*	--	N.F.*	--
NI	1000	Fail	--	Fail	--
GLD	1000	3.27	4.5	3.20	4.9
JSD	1000	3.15	0.8	3.30	7.5
GEV	1000	2.95	5.8	3.31	7.8

No failures.

Parallel System

Similar to the series system, Q was considered as the control variable. The exact

solution was obtained using $1x10^6$ MCS samples. It was observed that FS provided good

results for all low beta values. The GLD and GEV methods failed to provide any results

for the lognormal case. However, for the extreme I RV case, the GLD and the numerical

integration method produced close results to the exact solution whereas GEV failed to fit

the resistance samples. JSD provided good results for the lognormal RV case and failed

in the extreme I RV case. For the normal RV case with a load value Q of 40 kips, only

NI provided results, whereas all other methods failed to produce results.

Table 5.4. Parallel System with Normal RVs

mean load:		Q = 70		Q = 60		Q = 50		Q = 40	
method	no. calls	β	%err	β	%err	β	%err	β	%err
Exact Solution		-0.320	-	1.06	-	2.88	-	5.26	-
NI	1000	-0.321	0.09	1.04	2.0	2.85	1.1	5.36	1.9
MCS	1000	-0.362	13	1.01	5.0	2.65	7.9	N.F.	--
GLD	1000	-0.320	0.0	1.02	3.7	2.91	1.0	Fail	--
JSD	1000	-0.327	0.02	1.05	0.9	2.88	0.0	Fail	--
GEV	1000	-0.325	0.01	1.08	1.8	2.83	1.7	Fail	--

Table 5.5. Parallel System with Lognormal and Extreme I RVs

method	RVs: no. of calls	Lognormal β	%err	Extreme I β	%err
Exact Solution		3.53	-	3.57	--
MCS	1000	N.F.	--	N.F.	--
NI	1000	3.56	-0.8	3.40	0.8
GLD	1000	Fail	--	3.49	2.2
JSD	1000	3.55	0.28	Fail	--
GEV	1000	Fail	--	Fail	--

Minimum Function

Table 5.6. Minimum Function

Method	no. of calls	β	%err
Exact solution		2.28	--
FORM	--	2.33	2.15
MCS	1000	2.65	14.0
NI	1000	2.20	3.73
GLD	1000	2.27	0.31
JSD	1000	2.32	1.63
GEV	1000	2.42	5.42
Ensemble	1000	2.26	0.52

The results shown in Table 5.6 indicate that MCS failed to provide results with acceptable accuracy, while NI, JSD and GLD produced good results with low errors. However, GEV provided slightly high error. The ensemble of all FS methods proved to produce results of highest accuracy.

Maximum Function

The exact solution was obtained using 1×10^6 MCS samples. As shown in Table 5.7, FORM, GLD and GEV failed to provide any results, and MCS could not produce any failures. Here the ensemble produced results close to that of JSD. This can be attributed to the optimization of weights where JSD received the highest weight factor, and hence the ensemble approach provided almost the same result as JSD.

Table 5.7. Maximum Function

Method	no. of calls	β	%err
Exact solution		3.53	--
FORM	--	Fail	--
MCS	1000	N.F*	--
NI	1000	3.66	3.66
GLD	1000	Fail	--
JSD	1000	3.46	1.95
GEV	1000	Fail	--
Ensemble	1000	3.44	0.49

Multiple Reliability Indexes

FORM, GLD and GEV were unable to produce any results for this problem, and MCS was not able to produce any failures, as shown in Table 5.8. However, NI and JSD produced reasonable results, as did the ensemble approach.

Table 5.8. Multiple Reliability Indices

Method	no. of calls	β	%err
Exact solution		3.57	--
FORM	--	Fail	--
MCS	1000	N.F*	--
NI	1000	3.68	2.99
GLD	1000	Fail	--
JSD	1000	3.38	4.98
GEV	1000	Fail	--
Ensemble	1000	3.43	3.78

Circular Limit State

As shown in Tables 5.9 and 5.10, for the circular limit state function, the reliability indices for all cases were somewhat high. NI was the only method which produced results close to the exact solutions. JSD and the ensemble approach provided results only for the first case. In case where RVs were considered non-normal, it was observed that the ensemble approach further increased the accuracy of the results.

Table 5.9. Circular Limit State with Normal RVs

method	no. calls	radius: 4		5		6		7		8	
		B	%err	β	%err	β	%err	β	%err	β	%err
Exact Solution		3.40	--	4.48	--	5.54	--	6.58	--	7.62	--
MCS	1000	N.F.	--	N.F.	--	N.F.	--	N.F.	--	N.F.	--
NI	1000	3.38	0.7	4.53	1.3	5.56	0.4	6.60	0.3	7.57	0.7
GLD	1000	Fail	--	Fail	--	Fail	--	Fail	--	Fail	--
JSD	1000	3.53	3.7	Fail	--	Fail	--	Fail	--	Fail	--
GEV	1000	Fail	--	Fail	--	Fail	--	Fail	--	Fail	--
Ensemble	1000	3.46	1.73	Fail	--	Fail	--	Fail	--	Fail	--

Table 5.10. Circular Limit State with Non-Normal RVs

method	no. of calls	RVs: Lognormal		Extreme I	
		β	%err	β	%err
Exact Solution		3.42	--	3.29	--
MCS	1000	N.F.	--	N.F.	--
NI	1000	3.44	0.6	3.42	3.9
GLD	1000	Fail	--	Fail	--
JSD	1000	3.67	6.8	3.21	2.4
GEV	1000	3.33	2.7	Fail	--
Ensemble	1000	3.51	2.56	3.35	1.79

Analytical I-Beam

In this problem, all RVs were considered to be normal and independent, and P was considered as the control variable. The exact solution was obtained using 1×10^6 MCS samples. For the P control variable cases, it was observed that all methods provided good results for case 1 ($P = 6070$). However, for case 2 ($P = 14000$), as shown in Table 5.11, only NI, JSD and the ensemble approach were able to produce satisfactory results.

Table 5.11. Beam with Stress Limit State Functions

method	mean load P: no. of calls	6070 β	%err	14000 β	%err
Exact Solution		1.16	--	3.61	--
MCS	1000	1.17	0.8	N.F.	--
NI	1000	1.24	6.4	3.60	0.3
GLD	1000	1.06	8.6	Fail	--
JSD	1000	1.15	0.8	3.42	5.2
GEV	1000	1.16	0	Fail	--
Ensemble	1000	1.16	0	3.46	4.15

To further examine the effectiveness of GLD, the problem was re-examined with S taken as the control variable. Here, results were similar to the P control variable case, as shown in Table 5.12. The mean value of S was taken as 170000.

Table 5.12. Stress Limit State with 'S' as Control Variable

method	no. of calls	β	% err
Exact Solution		1.16	-
NI	1000	1.21	4.31
GLD	1000	1.12	3.44

Noisy Limit State

In this problem, it was desired to further examine the effectiveness of GLD. Here, the x_6 RV was considered as the control variable, with mean value of 40. As shown in Table 5.13, NI provided good results for this limit state function, while GLD provided slightly high error. The exact solution was taken from 1×10^6 MCS samples.

Table 5.13. Noisy Limit State

Method	No. of Calls	Beta	% Error
Exact Solution	1×10^6	2.25	-
NI	1000	2.22	1.33
GLD	1000	2.39	6.22

Realistic Practical Engineering Problems

10 Bar Nonlinear Static Truss

The exact solution was obtained from 1 x 10^5 MCS samples, which required approximately 400 CPU hours. These hours were shared between two processors. Tables 5.17 and 5.18 show the results obtained for the displacement and stress limit state functions, respectively. For the FS method, the number of function calls was restricted to 1000, whereas for a comparison FORM solution, this restriction was not applicable.

Table 5.17. Displacement Limit State Function of Non-linear Static Truss

method	nominal no. of calls	CPU time	mean P=65 β	%err	mean P=60 β	%err	mean P=50 β	%err
Exact Solution			1.554	-	2.25	--	3.59	--
FORM	150	2 hrs	1.370	11.8	1.96	12.9	3.12	13.1
MCS	1000	4 hrs	N.F.	--	N.F.	--	N.F.	--
NI	1000	5 hrs	1.44	7.33	2.18	3.11	2.57	28.4
GLD	1000	5 hrs	1.53	1.37	2.19	2.67	Fail	--
JSD	1000	5 hrs	1.59	2.14	2.28	1.05	3.61	0.41
GEV	1000	5 hrs	1.56	0.64	2.34	3.85	Fail	--

In the tables, it can be observed that the FS method provided good results for almost all cases. GEV performed well for low and moderate beta values but failed to produce results for the high beta case. In the high beta cases ($\beta = 3.59$ and 3.79), for the displacement and stress limit states, the error due to NI (28.4% and 16.3%) exceeded an

assumed acceptable limit of 5%. FORM either resulted in high errors or failed to provide any results, indicating that this problem is particularly suited for the FS method, as reliability-index reliability methods are unsuitable here. Moreover, for the given number of function calls, MCS could not provide a solution. FS paired with JSD provided good results in all cases. Overall, FS provided good results with errors generally within reasonable limits.

Table 5.18. Stress Limit State Function of Non-linear Static Truss

Method	nominal no. of calls	CPU time	mean P = 55		mean P = 45	
			β	%err	β	%err
Exact Solution			1.78	--	3.79	--
FORM	150	2 hrs	Fail	--	Fail	--
MCS	1000	4 hrs	N.F.	--	N.F.	--
NI	1000	5 hrs	1.86	4.30	3.17	16.3
GLD	1000	5 hrs	1.79	0.83	Fail	--
JSD	1000	5 hrs	1.75	1.46	3.82	0.78
GEV	1000	5 hrs	1.73	2.76	Fail	--

Steel Frame Structure

All RVs were considered normally distributed. The limit state function was evaluated using ABAQUS (Version 6.11-2). Pressure load was considered to be the control variable. Approximately 600 CPU hours were required for 1×10^5 MCS samples to

evaluate the exact solution. Results are shown in Table 5.19. For the lower beta case (1.803), all FS implementation methods, as well as FORM and MCS, produced results with reasonable error. However, for the higher beta case (3.26) only GLD and JSD were able to fit to the resistance sample, with JSD providing reasonable results of less than 4% error. As FORM and MCS were unable to produce solutions, this problem is also clearly suited for the FS approach.

Table 5.19. Steel Frame Structure

method	Nominal no. of calls	CPU time	mean P = 70 β	%err	mean P = 90 β	%err
Exact Solution			1.803	--	3.26	--
FORM	150	3 hrs	1.86	3.27	Fail	--
MCS	1000	6 hrs	1.82	0.93	N.F.	--
NI	1000	5 hrs	1.84	2.01	Fail	--
GLD	1000	5 hrs	1.89	4.85	3.52	7.38
JSD	1000	5 hrs	1.76	2.55	3.14	3.68
GEV	1000	5 hrs	1.82	0.44	Fail	--

Metal Automotive Structure

As mentioned earlier the crash scenario analyzed with the Bogie model is a small car impacting a rigid pole. Here, the simulated nose structure is considered for low speed impacts (32 km/hr). For the reliability analysis, failure is in terms of material failure in the honeycomb nose structure. Specifically, failure was defined as an event where the

stress in any element of the honeycomb nose structure exceeded its yield stress. Alternatively, failure can be defined in terms of deformation of the nose structure. Figures 5.17, 5.18 and 5.19 show the model before and after a representative impact. All RVs were considered normally distributed. The crash analysis was conducted with LS-Dyna and LS-Prepost Version 4.1. Young's modulus was considered as the control variable. As shown in Table 5.20, MCS was unable to record any failures, while FORM was also unable to generate any results. The NI and GLD implementation approaches of FS were found to have higher errors than JSD, which was found to have reasonably small error.

Table 5.20. Results for Metal Automotive Structure Problem

Method	Implementation Methods	Function Calls	Beta	% error
Exact		10^8	2.82	-
FS_MCS	NI	1000	3.08	8.44
	GLD		2.66	5.67
	JSD		2.72	3.55
	GEV		Fail	-
MCS		1000	N.F.**	-
FORM	HL-RF*	-	Fail	-

*Hasofer Lind – Rackwitz Fiessler   **N.F. – No Failures*
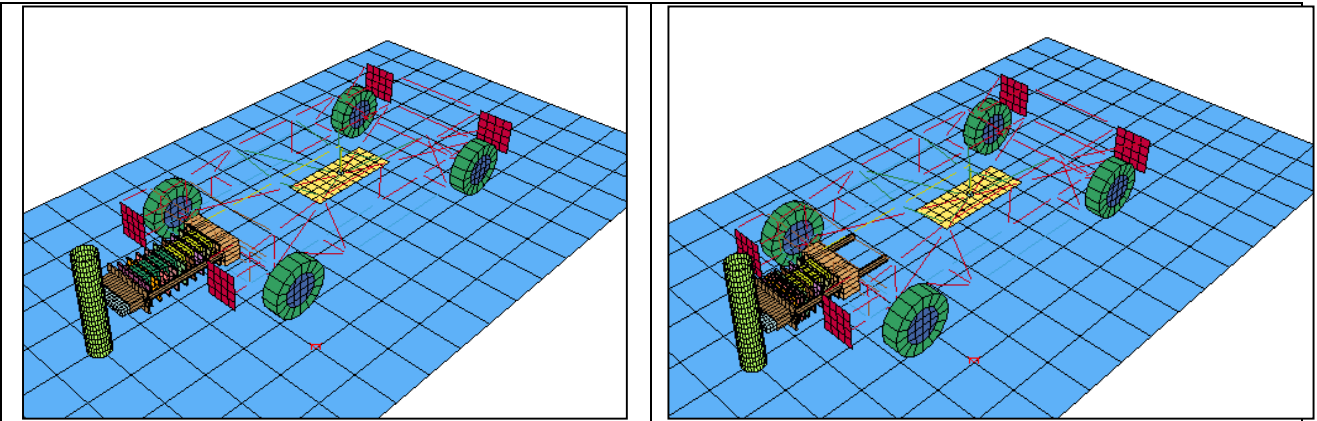
Figure 5.17. Bogie Model Before and After Impact
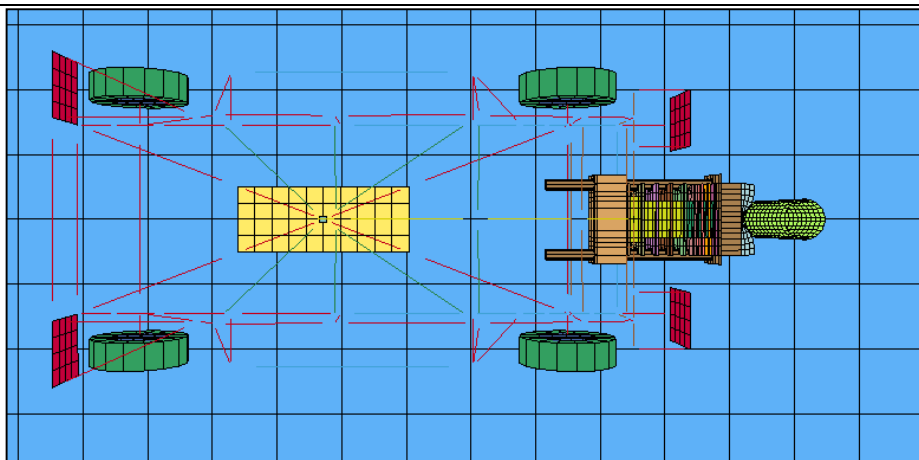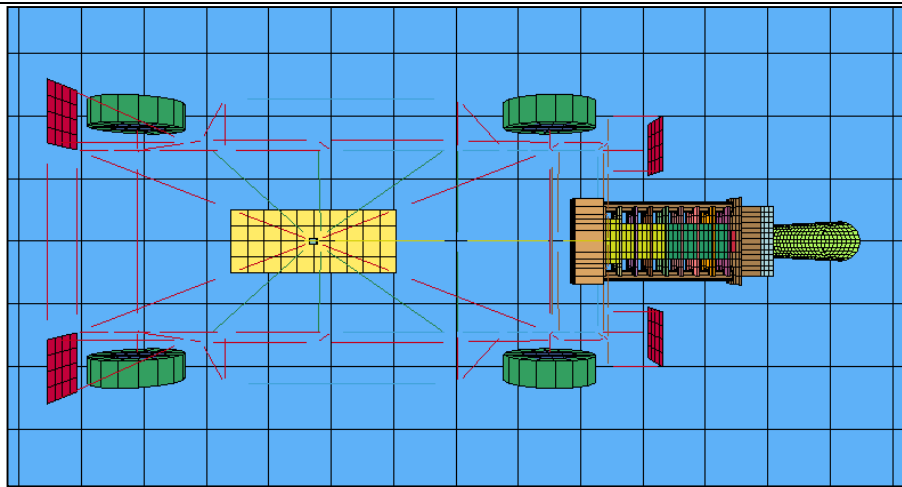
Figure 5.18. Bogie Nose Structure Before and After Impact
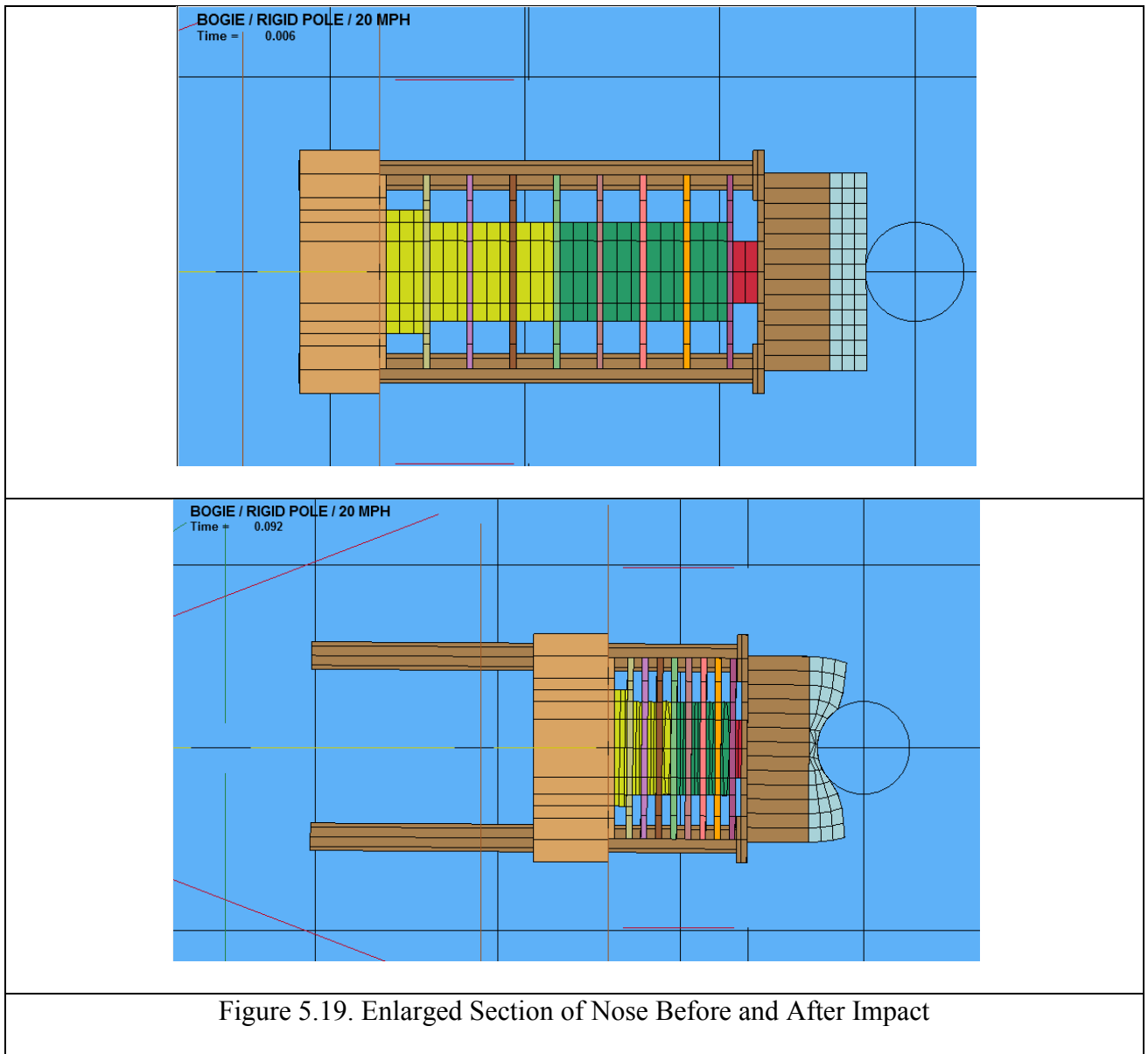
Figure 5.19. Enlarged Section of Nose Before and After Impact

Marine Structure

The resistance RVs considered for this problem were steel material properties whereas the waveslab load was considered as the load RV for this problem. All RVs are assumed to have normal distributions. The limit state is expressed in terms of strain, and in exceeded when the tensile strain in any of the stiffeners exceeds an allowable value, or if the strain in steel crown reaches an allowable Von Mises strain ε_{stmax} (Rais-Rohani et al 2006). The problem is solved using FS, MCS & FORM with 1 x 10^9 MCS samples producing the exact solution. As seen from results in Table 11, FORM failed to produce any results whereas MCS with 1000 function calls failed to generate any failures. However, FS produce reasonably accurate results with most of its implementation methods.

Table 5.21. Results for Marine Structure

Method	Implementation Methods	Function Calls	Beta	% error
Exact		10^9	3.03	-
FS_MCS	NI	1000	3.22	5.90
	GLD		3.14	3.50
	JSD		3.20	5.31
	GEV		Fail	-
MCS	Standalone	1000	N.F.**	-
FORM	HL-RF*	-	Fail	-

*Hasofer Lind – Rackwitz Fiessler   **N.F. – No Failures*
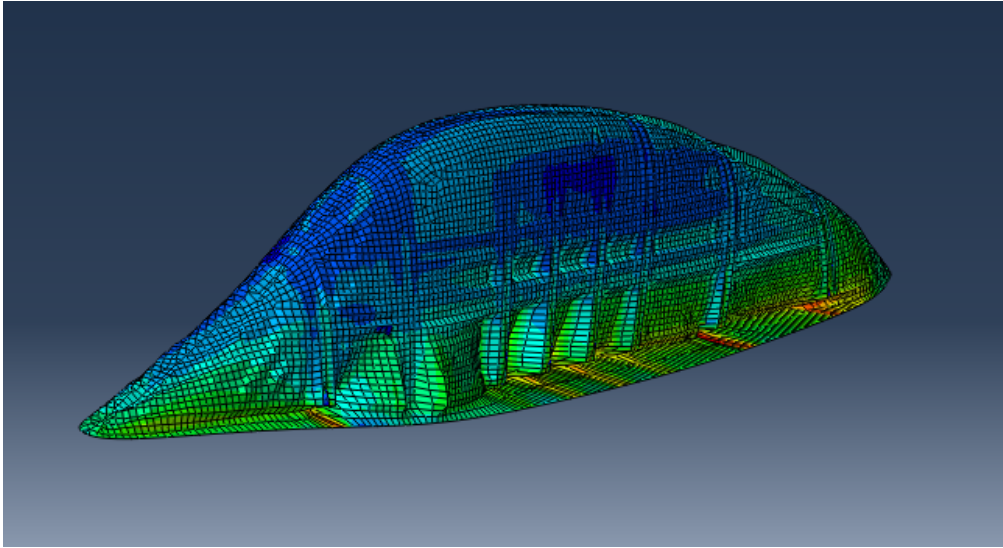
Figure 5.20 Stresses in Marine Sail Structure

Masonry Building Structure

Figure 5.21 shows two alternative modes of deformation (out of many possible, depending on the realized values of the RVs in the simulation) at a selected instant of time in the analysis.   All RVs were considered normally distributed. The limit state function was evaluated using ABAQUS (Version 6.11-2). Peak pressure load was considered as the control variable. The exact solution was computed using 1×10^9 MCS samples. The problem was evaluated using FORM, MCS and FS. Results are given in Table 5.22. As shown in the table, MCS with 1000 function calls was unable to record any failure, while FORM failed to produce acceptably accurate results. On the other hand, FS coupled with JSD and NI produced reasonably accurate results.

Table 5.22. Results for Masonry Building Structure Problem

Method	Implementation Methods	Function Calls	Beta	% error
Exact		10^9	3.16	-
FS_MCS	NI	1000	3.23	2.17
	GLD		Fail	-
	JSD		3.30	4.24
	GEV		Fail	-
MCS	Standalone	1000	N.F.**	-
FORM	HL-RF*	-	1.98	37.34

*Hasofer Lind – Rackwitz Fiessler **N.F. – No Failures*

Figure 5.21 Alternative Failed States
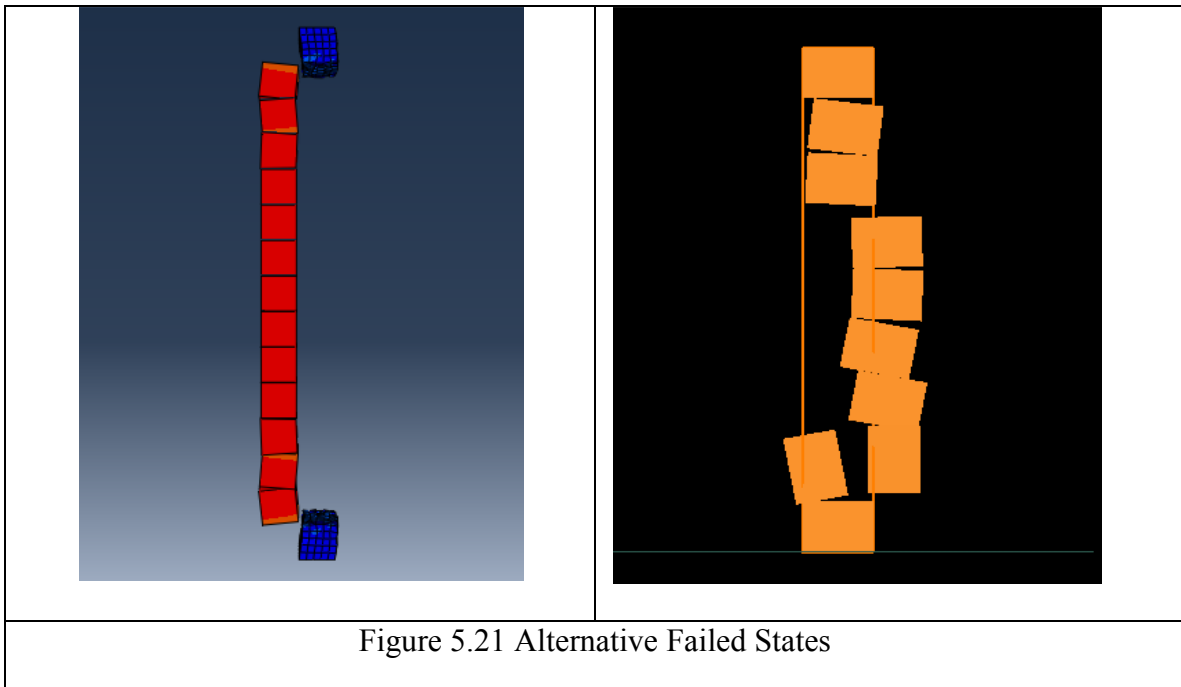
Effect of MCMC On Generation of *R(Xᵢ)* Samples

The MCMC method is explored in lieu of crude MCS to generate the resistance sample $R(X_i)$. The objective is to make an attempt to further reduce the number of data (below 1000) to reduce computational costs.

A selection of the limit state functions described in Chapter 4 were solved using the FS-MCMC approach. These results are presented in the following tables that compare the computational effort required by FS-MCS, FS-MCMC, and traditional simulation methods, as well as beta-based methods.

Circular Limit State Function

The limit state function is described in detail in Chapter 4. The problem is solved using crude MCS, MCMC, FORM and the FS method. The problem is solved with the FS method twice; once by generating resistance samples using MCS, and again by MCMC. Further, two sample sizes of resistance for FS were considered. In the first case, 1000 resistance data were generated, while in the second case, the sample size was decreased until an acceptable level of accuracy (taken as a maximum error in reliability index of 5%) was unachievable. The results are given in Tables 5.23 and 5.24. It can be observed that the GLD was the only distribution which could not be fit to the resistance samples, and use of 1000 resistance data using MCS and MCMC produced good results for most of the FS implementation techniques. It was also found that, using MCMC, the resistance sample size could be reduced to 700 without significant loss of accuracy. On the other hand, FORM produced relatively high errors whereas MCS and MCMC, when

used as standalone methods and evaluated for the same number of function calls as of FS, were unable to record any failures.

Table 5.23. Results for Circular Limit State Function

Method	Implementation Methods	Function Calls	Beta	% error
Exact	-	-	3.401	-
MCS	Standalone	10^6	3.412	0.335
MCMC	Standalone	10^6	3.412	0.335
FS_MCS	NI	1000	3.377	0.706
	GLD		Fail	-
	JSD		3.284	3.440
	GEV		3.574	5.074
FS_MCMC	NI	1000	3.503	3.014
	GLD		Fail	-
	JSD		3.450	1.446
	GEV		3.560	4.680
MCS	Standalone	1000	N.F.*	-
MCMC	Standalone	1000	N.F.*	-
FORM	HL-RF**	24	4.000	17.61

*No Failures   **Hasofer Lind – Rackwitz Fiessler*

Table 5.24. Results for Circular Limit State Function

Method	Implementation Methods	Function Calls	Beta	% error
Exact	-	-	3.401	-
FS_MCS	NI		2.856	16.024
	GLD		Fail	-
	JSD	700	3.652	7.386
	GEV		3.724	9.500
FS_MCMC	NI		3.270	3.845
	GLD		Fail	-
	JSD	700	3.515	3.346
	GEV		3.762	10.614
MCS	Standalone	700	N.F.*	-
MCMC	Standalone	700	N.F.*	-
FORM	HL-RF**	24	4.000	17.61

*No Failures   **Hasofer Lind – Rackwitz Fiessler*

Analytical I-Beam

This problem is described in Chapter 4. Similar to the circular limit state, this problem was evaluated using FS, FORM, MCS and MCMC. The results considering two different mean load levels (P), to vary the reliability index, are shown in Tables 5.25 and 5.26. The exact solutions were obtained from 10^6 and 10^9 crude MCS samples for each case, respectively. For the lower reliability index case (Table 5.25), it can be seen that FS

with MCMC produced nearly equivalent or higher accuracy while using fewer resistance data as compared to FS with crude MCS. Further, it was observed that using JSD to implement FS produced the most accurate results for both MCS and MCMC. For the higher reliability index case however, consistent and accurate results were obtained only from FS coupled with JSD, and some cases of FS with NI. Moreover, higher accuracy was obtained by using MCMC with FS as compared to using MCS. Further, when the number of function calls was decreased from 1000 to 700, it was observed that FS coupled with MCMC and JSD were the only case producing results of acceptable accuracy. The standalone crude MCS and MCMC methods failed to produce any results when allowed to run for the same number of function calls as FS, whereas FORM produced results of unacceptable accuracy as well.

Table 5.25. Results for Simple I-beam with P (6070, 200)

Method	Implementation Methods	Function Calls	Beta	% error
Exact		10^6	1.131	-
FS_MCS	NI	1000	1.139	0.219
	GLD		1.072	5.212
	JSD		1.088	3.802
	GEV		1.083	4.244
FS_MCMC	NI	700	1.091	3.534
	GLD		1.101	2.652
	JSD		1.127	0.354
	GEV		1.080	4.509
MCS	Standalone	1000	1.039	8.134
MCMC	Standalone	1000	1.042	7.869
FORM	HL-RF*	50	1.045	7.604

Table 5.26. Results for Simple I-beam with P (14000, 460.6)

Method	Implementation Methods	Function Calls	Beta	% error
Exact		10^9	3.644	-
FS_MCS	NI	1000	3.840	5.384
	GLD		Fail	-
	JSD		3.694	1.394
	GEV		Fail	-
FS_MCMC	NI	1000	3.582	1.701
	GLD		N.F.**	-
	JSD		3.652	0.225
	GEV		Fail	-
FS_MCS	NI	700	3.149	13.584
	JSD		3.238	11.142
FS_MCMC	NI	700	3.352	8.013
	JSD		3.808	4.503
MCS	Standalone	1000	N.F.**	-
MCMC	Standalone	1000	N.F.**	-
FORM	HL-RF*	483	7.591	108.28

*Hasofer Lind – Rackwitz Fiessler   **N.F. – No Failures*

CHAPTER 6 CONCLUSIONS AND RECOMMENDATIONS

In this research, the Advanced Failure Sampling method was developed. It was found superior to the FS approach and useful for complex, computationally demanding reliability problems for which traditional methods may provide unacceptably inaccurate or unfeasibly computationally costly solutions.

Summary and Conclusion

This research was divided in to two major tasks, method development and method validation. The development task focused on formulating the Advanced FS Method. In this task, optimal algorithm for probability density function (PDF) construction from sampled resistance ($R(x)$) data, in terms of selection of interval size was determined. A thorough examination of over 96 different limit state functions found that an interval size of 50 for 1000 resistance samples consistently provided good results with highest accuracy, and is recommended for use in the Advanced FS Method.

Next, in addition to this numerical integration approach, an alternative procedure for determining probability of failure by using analytical curve fits was further developed. The distributions considered were the Generalized Lambda Distribution (GLD), the Extended Generalized Lambda Distribution (EGLD), Johnsons Distribution (JSD) and the Generalized Extreme Value Distribution (GEV). It was found that the FS method coupled with JSD produced the most accurate and consistent results for most of the analytical limit state functions considered. Some additional findings of interest are as follows. Although JSD was generally the most accurate and precise, for limit state functions having 15 random variables (RV) and a high reliability index (β), JSD

produced low precision results. GEV failed to produce any results for high reliability cases, and for 15 RV, highly non-linear cases with low target reliability indices, it produced low precision results. GLD failed to produce results for the high reliability cases, but there was no specific pattern for the accuracy or precision of the results obtained for the remaining test cases. The NI method produced poor results for most of the lognormal distributions, and its precision was somewhat degraded. In summary, the JSD implementation is generally most effective, but not in all cases.   Further,   a procedure to develop an optimal probability density function (PDF) of the resistance sample for the Advanced FS Method using a design ensemble optimization technique was explored. This approach uses an ensemble of PDFs obtained from NI and the curve fit methods in order to find their respective optimized weight factors. The PDFs along with their respective weight factors were then combined to construct the optimal PDF. It was observed that the optimized ensemble further reduced the lowest effective error (obtained from finding the minimum of errors due to JSD, GLD & GEV) in most cases, and was found to be more effective than the use of a single curve alone. In a few cases, an insignificant difference was observed between the lowest effective error and the error obtained from ensemble technique. In summary, the optimal ensemble approach as developed is recommended for use in the Enhanced FS approach.

Further, the integration of MCMC within FS was explored, with the intent to further reduce the computational effort required. In general, it was observed that the FS method with different curve fitting techniques coupled with MCMC provided accurate and consistent results with the least computational effort over the alternative approaches.

It was also observed that the resistance part of the limit state function was better represented by the MCMC technique as compared to MCS in the FS approach. In general, the use of MCMC is recommended over MCS in the Advanced FS Method.

In summary, the Advanced FS Method involves: 1) general use of a 50-interval PDF for a sample size of 1000; 2) the optimal ensemble approach for construction of the PDF of the resistance sample, and; 3) the use of MCMC to sample resistance.

Task 2 of this research involved model validation. In this task, various complex problems involving FEA were considered for evaluation of the limit state function. These problems included a nonlinear truss, a nonlinear steel frame structure, a metal automotive structure, a composite marine structure, and a masonry building structure, based on existing complex engineering problems in the literature. The latter three problems were most complex, and computationally expensive. For the steel frame and metal automotive structure problems, results indicated that the JSD approach resulted in lowest error between 3-4%, while traditional methods (FORM, MCS) could provide no solutions for the same computational effort. For the marine structure, the GLD approach gave best results at 3.5% error, with NI and JSD provided solutions with 5-6% error, while traditional methods (FORM, MCS) could provide no solutions with the same computational effort. For the masonry wall problem, NI and JSD provided solutions with 1000 simulations at 2-4% error, while MCS provided no solutions and FORM resulted in 37% error. Therefore, it is concluded that the FS approach and the general recommendation to use JSD was successfully validated for the complex engineering problems considered.

Recommendations for Future Research

The following areas of investigation are recommended for further development of the FS method:

1. Explore possible integration of subset simulation with the Advanced FS Method for $R(X_i)$ sample generation and determine if the sample size can further be reduced while maintaining accuracy.

2. Investigate inclusion of additional methods in the optimized ensemble to develop PDF of resistance such as a response surface technique.

3. In an effort to further reduce computational effort, explore and integrate the use of more advanced root finding methods to solve for the value of the control variable during resistance sample generation for implicit nonlinear limit state functions.

4. Determine the optimal number of intervals for different resistance sample sizes.

REFERENCES

AASHTO LRFD Bridge Design Specifications, 5th ed. American Association of State and Highway Transportation Officials, Washington, DC, 2010.

Acar, E., Rais-Rohani M., and Eamon C. D., "Reliability Estimation Using Dimension Reduction   and Extended Generalized Lambda Distribution," *American Institute of Aeronautics and   Astronautics, Inc.,* April 2008, pp 1-15.

ACI 318-08: Building Code Requirements for Structural Concrete. American Concrete Institute,   Farmington Hills, MI, 2008.

Agarwal, H., Mozumder, C.K., Renaud, J.E. and Watson, L.T. "An inverse-measure-based unilevel architecture for reliability-based design optimization.' Structural and   Multidisciplinary Optimization, Vol. 33, No. 3, pp. 217–227, 2007.

ANSI/AISC 360-05: Specifications for Structural Steel Buildings. American Institute of Steel   Construction, Chicago, IL., 2005.

ASCE 7-10: *Minimum Design Loads for Buildings and Other Structures*. American Society of   Civil Engineers, Reston, VA,, 2010.

Asif, L. and Helmut, M. "Estimating the Parameters of the Generalized Lambda Distribution." ALGO Research Quarterly, pp. 47-58, 2000

Au, S.K. and Beck, J.L. "Estimation of small failure probabilities in high dimensions by subset simulation." Probabilistic Engineering Mechanics, Vol. 16, pp 263-277, 2001.

Ayyub, B.M., and Haldar, A. "Practical Structural Reliability Techniques." ASCE Journal of   Structural Engineering, Vol. 110, No. 8, pp. 1707-1724, 1984.

Au, S.K., Ching, J. and Beck, J.L. "Application of subset simulation methods to reliability benchmark problems." Structural Safety, Vol. 29, pp 183-193, 2007.

Breitung, K. "Asymptotic Approximations for Multinormal Integrals." Journal of Engineering Mechanics, ASCE, Vol. 110, No. 3, pp 357-366, 1984.

Bucher, C.G. and Bourgund, U. "Fast and efficient response surface approach for structural reliability problems." Structural Safety, Vol. 7, No. 1, pp. 57-66, 1990.

Chen, X. and Lind, N.C. "Fast Probability Integration by Three-Parameter Normal Tail Approximation." Structural Safety, Vol. 1, pp. 269-276, 1983.

Charumas B., "A New Technique for Structural Reliability Analysis," *MSC Thesis*, Department of Civil and Environmental Engineering, Mississippi State University, May 2008.

Cheng, J. and Li, Q.S. "Application of Response Surface Methods to Solve Inverse Reliability Problems with Implicit Response Functions." Computers and Mechanical, Vol. 43, pp. 451-459, 2009.

Chiralaksanakul, A. and Mahadevan, S. "First-Order Methods for Reliability-Based Optimization." ASME Journal of Mechanical Design, Vol. 127, No. 5, pp. 851-857, 2005.

Choi, K.K., Tu, J. and Park, Y.H. "Extensions of design potential concept for reliability-based design optimization to nonsmooth and extreme cases." Structural and Multidisciplinary Optimization, Vol. 22, pp. 335–350, 2001.

Der Kiureghian, A., Lin, H.Z., and Hwang, S.J. "Second-Order Reliability Approximations," ASCE Journal of Engineering Mechanics, Vol. 113, No. 8, pp. 1208-1225, 1987.

Ditlevsen, O, Olesen, R., Mohr, G. "Solution of a Class of Load Combination Problems by Directional Simulation." Structural Safety, Vol. 4, No. 2, pp. 95-109, 1987.

Dudewicz E. J., and Karian Z. A., "EGLD System For Fitting Distributions to Data With Moments, II: Tables," *American Journal of Mathematical and Management Sciences*, 1996, Vol 16, Issue 3-4, pp 271-332.

Eamon C.D., and Charumas B., "Reliability estimation of complex numerical problems using modified conditional expectation method," *Computers and Structures 89*, October 2010, pp 181-188.

Eamon, C. "Reliability of Concrete Masonry Unit Walls Subjected to Explosive Loads," Journal of Structural Engineering, Vol. 133, pp. 1-10.

Eamon, C. and Rais-Rohani, M. "Integrated Reliability & Sizing Optimization of Large Composite Structure." Marine Structures, Vol 22, pp 315-334, 2008.

Eamon, C. 'Reliability of Concrete Masonry Unit Walls Subjected to Explosive Loads' Journal of Structural Engineering, pp 1-10, 2007

Eamon, C., Thompson, M., and Liu, Z. "Evaluation of Accuracy and Efficiency of some Simulation and Sampling Methods in Structural Reliability Analysis," Journal of Structural Safety, Vol. 27 No. 4, pp. 356-392, 2005.

Ellingwood, B. Galambos, T.V., MacGregor, J.C., and Cornell, C.A. "Development of a Probability Based Load Criteria for American National Standard A58." NBS Special Publication No. 577, National Bureau of Standards, US Dept. of Commerce, Washington, DC, 1980.

Engelund, S. and Rackwitz, R. "A benchmark study on importance sampling techniques in structural reliability, Structural Safety, Vol. 12, No. 4, pp. 255-276, 1993.

Fiessler, B., Neumann, H.J., and Rackwitz, R. "Quadratic Limit States in Structural Reliability." ASCE Journal of Engineering Mechanics, Vol. 1095, No. 4, pp. 661-676, 1979.

Furuta, H., Miyake, K. and Tsukiyama, I. (2010) "Reliability Analysis of Lifeline Network Using Markov-Chain Monte Carlo Simulation." ASRANet Conference, 2010.

Galambos, T.V. and Ravindra, M.K. "Properties of Steel for Use in LRFD." ASCE Journal of the Structural Division, Vol. 104, No. 9, pp. 1459-1468, 1978.

George, F. "Johnsons System of Distribution and Microarray Data Analysis." PhD Thesis Dissertation, Department of Mathematics, University of South Florida, 2007.

Gomes, H.M. and Awruch, A.M. "Comparison of Response Surface and Neural Network with Other Methods for Structural Reliability Analysis." Structural Safety, Vol. 26, pp. 49-67, 2004.

Guan, X.L. and Melchers, R.E. "Load Space Formulation for Probabilistic Finite Element Analysis of Structural Reliability." Probabilistic Engineering Mechanics, Vol. 14, No. 1- 2, pp. 73-81, 1999.

Haldar, A. and Mahadevan, S. Probability, Reliability, and Statistical Methods in Engineering Design, John Wiley & Sons, New York, 2000.

Hohenbichler, M., Gollwitzer, S., Kruse, W., and Rackwitz, R. "New Light on First- and Second-Order Reliability Methods." Structural Safety, Vol. 4, pp. 267-284, 1987.

Iman, R.L. and Conover, W.J. "A distribution-free approach to inducing rank correlation among input variables." Communications in Statistics Vol. 11, No. 3, pp 311-334, 1982.

Karamchandani, A., Bjerager, P., and Cornell, A.C. "Adaptive Importance Sampling." Proceedings, International Conference on Structural Safety and Reliability (ICOSSAR), San Francisco, CA., pp. 855-862, 1989.

Karian Z.A., and Dudewicz E. J., "Handbook of Fitting Statistical Distributions with R," CRC Press, 2010.

Kharmanda, G., Olhoff, N. and El-Hami, A. "Optimum values of structural safety factors for a predefined reliability level with extension to multiple limit states." Structural and Multidisciplinary Optimization, Vol. 27, No. 6, pp. 421–434, 2004.

Lee, H. and Kwak, M. "Reliability-based structural optimal design using the Neumann expansion technique." Computers and Structures, Vol. 55, No. 2, pp. 287–296, 1995.

Melchers, R.E. Structural Reliability Analysis and Prediction, 2nd ed. John Wiley & Sons, New York, 1999.

Nowak, A.S. and Collins, K.R. *Reliability of Structures*, McGraw Hill, New York, 2000.

Nowak, A.S. and Szerszen, M.M. "Calibration of design code for buildings (ACI 318): Part 1 - Statistical models for resistance." *ACI Structural Journal*, Vol. 100, No. 3, 2003.

Ozaturk, A. and R. F. Dale. "A study of Fitting the Generalized Lambda Distribution to Solar   Radiation Data." American Meteorological Society, July, 1982.

Rackwitz, R. and Fiessler, B. "Structural Reliability Under Combined Random Load Sequences." Computers and Structures, Vol. 9, No. 5, pp. 484-494, 1978.

Rais-Rohani, M, Solanki, K, Acar, E., and Eamon, C. "Shape and Sizing Optimization of Automotive Structures with Deterministic and Probabilistic Design Constraints," International Journal of Vehicle Design, Vol. 54, No. 4, pp. 309-338, 2010.

Rosowsky, D., Gromala, D.S., and Line, P. "Reliability Based Code Calibration of Wood Members Using Load and Resistance Factor Design."   ASCE Journal of Structural Engineering, Vol. 131, No. 2, pp. 338-344, 2005.

Rubinstein, R.Y. *Simulation and the Monte Carlo Method*, John Wiley & Sons, New York, 1981.

Slifker, J.F. and Shapiro, S.S. "The Johnson System: Selection and Parameter Estimation." Technometrics, Vol. 22, No. 2, pp. 239-246, 1980.

Steyvers, M. "Computational Statistics with Matlab.", 2011.

Tvedt, L. "Distribution of Quadratic Forms in Normal Space--Application to Structural Reliability."   ASCE Journal of Engineering Mechanics, Vol. 116, No. 6, pp. 1183-1197, 1990.

Venkatraman, S. and Haftka, R.T. "Structural Optimization Complexity: what has Morre's law done for us?" Structural and Multidisciplinary Optimization, Vol. 28, pp. 375-387, 2004.

Wu, Y.T. "An Adaptive Importance Sampling Method for Structural Systems Analysis, Reliability Technology 1992." Edited by T.A. Cruse, ASME Winter Annual Meeting, Vol. AD 28. Anaheim, CA, pp. 217-231, 1992.

Wu, Y.T., and Wirsching, P.H. "New Algorithm for Structural Reliability Estimation." Journal of Engineering Mechanics, ASCE, Vol. 113, No. 9, pp. 1319-1336, 1987.

Yang, R.J. and Gu, L. "Experience with approximate reliability-based optimization methods." Structural and Multidisciplinary Optimization, Vol. 26, No. 1–2, pp.152–159, 2004.

Zou, T. and Mahadevan, S. "A direct coupling approach for efficient reliability-based design optimization." Structural and Multidisciplinary Optimization, Vol. 31, No. 3, pp.190–200, 2006.

ABSTRACT

ACCURATE AND EFFIFICIENT RELIABILITY ANALYSIS OF COMPLEX STRUCTURAL ENGINEERING PROBLEMS

by

KAPIL DILIP PATKI

December 2015

Advisor: Dr. Christopher Douglas Eamon

Major: Civil Engineering

Degree: Doctor of Philosophy

Accurate probabilistic analysis of complex engineering problems with reasonable computational effort is a popular area of research in structural reliability analysis. For probabilistically complex problems such as those involving nonlinear FE analysis; traditional simulation methods often require unfeasibly great computational effort, while low-cost reliability index approaches may lack sufficient accuracy. This dissertation report addresses this issue by developing a simulation-based method referred to as Advanced Failure Sampling (FS).

In this research, the Advanced FS Method is developed with an objective to solve complex structural reliability problems with reasonable computational effort. In order to achieve this, a thorough evaluation of this method is conducted. This research report suggests and explores various techniques needed to implement to transform the existing FS method into a complete, robust algorithm for reliability analysis; the Enhanced FS approach. These enhancements include: developing an optimal algorithm for construction of probability density function (PDF) of resistance samples; determining a more efficient

way to simulate the resistance samples; and determining the optimal interval size for a typical resistance sample size of 1000. The process of developing an optimal algorithm for constructing a PDF estimate of the resistance sampls included exploring the use of various curve-fit methods and developing an optimized ensemble technique to maximize accuracy of the failure probability calculation. The Markov Chain Monte Carlo method was investigated with an aim to further reduce the computational effort of FS. Moreover, to evaluate the effectiveness of these suggestions, a database of test problems is described and presented in this report. These problems are solved with the FS method using the different techniques suggested above to guide and validate formulation of the Enhanced FS approach. The test problems include a wide variety of limit states that were designed to consider different parameters of interest such as: number of random variables (RVs); degree of nonlinearity; level of variance; and type of RV probability distribution. The method was also validated further for complex realistic engineering problems requiring finite element analysis. The results obtained from the research indicate that significantly better results for a wide variety of problems can be obtained when FS is implemented with a curve fit technique using the JSD distribution; in the Enhanced FS approach, rather than the NI and GLD methods as originally implemented in FS. It was found that the Advanced FS Method has the capabilities of producing accurate and efficient results for complex, computationally demanding reliability problems for which traditional methods may provide unacceptably inaccurate or unfeasibly computationally costly solutions.

AUTOBIOGRAPHICAL STATEMENT

Structural engineering has always fascinated me as a student. Hence, after completing my under graduation in Civil Engineering and gaining a couple years of work experience in India, I decided to study further. I arrived in United States in 2007 to pursue my Masters in Civil Engineering at Lawrence Technological University (LTU), Southfield, MI and was offered a research assistantship position to study the flexural behavior of side-by-side box-beams reinforced with carbon fiber composite cable. I completed my Masters program in 2010 and was offered a Structural Engineer position at GPD Group in Ohio where I worked for a year. However, I always wanted to pursue my research and academic interest in Structural engineering further. During my master's at LTU I had seen a presentation on 'Structural Reliability' which developed curiosity and interest about this particular field. I applied at Wayne State University for PhD graduate studies and expressed my desire to work in structural reliability analysis field towards Dr. Christopher Eamon. I was fortunate to receive a Thomas Rumble fellowship and research assistantship to work on my research topic 'Accurate and Efficient Reliability Analysis of Complex Structural Engineering Problems' under the guidance of Dr. Christopher Eamon. I am currently working at at J3 Engineering Group, LLC as a Project Engineer. After completing my PhD, I want to continue my research in the field of structural reliability further along with an aim to pursue a career in academics.